

Department of Biomedical Sciences
University of Veterinary Medicine Vienna

Institute of Pharmacology and Toxicology
(Head: Univ.-Prof. Dr.med.univ. Veronika Sexl)

Antileishmanial Action of Endoperoxides

Bachelor thesis submitted for the fulfilment of the requirements for the degree of
Bachelor of Science (BSc.)

University of Veterinary Medicine Vienna

submitted by

Sara Todhe

Vienna, June 2021

All experiments for this thesis were conducted from February to May 2021 in the group and under the supervision of Ao. Univ.-Prof. Dr.rer.nat. Lars Gille at the Institute of Pharmacology and Toxicology in the Department of Biomedical Sciences.

Reviewer: Dipl.-Biol. Dr.rer.nat. Catharina Duvigneau
University of Veterinary Medicine Vienna
Department of Biomedical Sciences
Institute for Medical Biochemistry
Veterinärplatz 1
1210 Vienna

Acknowledgements

I would like to thank the following important people who have supported me during my bachelor's degree and Thesis.

Firstly, I would like to express my gratitude to my supervisor Ao.Univ.-Prof. Dr.rer.nat. Lars Gille for giving me the opportunity to carry out this thesis and for unfaltering support, insight, and guidance through my work.

I want to express my gratitude to Mag. Laura Machin Galarza for helping me with my practical work.

Furthermore, I sincerely thank to Ao.Univ.-Profⁱⁿ Drⁱⁿ rer.nat. Katrin Staniek and Anja Maria Holzer for creating a great work environment.

Last but not least, I acknowledge the financial support for this work by the Austrian Science Fund (FWF) under grant P 27814-B22.

Table of contents

1. Introduction	1
1.1 Leishmaniasis	1
1.1.1 Epidemiology	1
1.2 <i>Leishmania</i>	3
1.2.1 Life cycle of <i>Leishmania</i>	4
1.2.2 <i>Leishmania</i> -macrophage interaction	5
1.3 Treatments against leishmaniasis	6
1.3.1 Vaccine candidates	7
1.3.2 Pentavalent antimonials	7
1.3.3 Amphotericin B	8
1.3.4 Pentamidine	8
1.3.5 Paromomycin	9
1.3.6 Miltefosine	9
1.3.7 Combination therapy	9
1.4 Endoperoxides	10
1.4.1 Effects of endoperoxides in <i>Leishmania</i>	10
1.5 Test systems	11
1.5.1 <i>In vitro</i>	11
1.5.2. <i>In vivo</i>	12
1.6 Viability assays	13
1.7 Aims of the study	14
2. Materials and Methods	15
2.1 Chemicals	15
2.2 Endoperoxides and analogues	16
2.3 Cell culture	18
2.3.1 LtP cell culture	18
2.3.2 J774 macrophage cell culture	18
2.4 Viability assays	18

2.4.1 Viability assay for LtP	18
2.4.2 Viability assay for J774 macrophages.....	21
2.5 UV detection of cycloreversion in AcEPs.....	22
2.6 Formation of the xylenol/Fe ³⁺ complex by EP	22
2.7 Detection of superoxide radicals by CMH/EPR	23
2.8. Data analysis	23
3. Results	24
3.1 Method development	24
3.1.1. Single compound assays.....	24
3.1.2. Combination viability assay	24
3.2 Influence of EPs and non-EPs on viability of LtP and J774	26
3.3 Measurement of superoxide radicals by CMH/EPR.....	27
3.4 Chemical reaction mechanisms of AcEPs	31
3.4.1 Reactivity of EP with FeSO ₄	31
3.4.2 UV detection of cycloreversion	32
4. Discussion	39
5. Summary	43
6. Zusammenfassung.....	44
7. Abbreviations	46
8. References	48
9. List of figures.....	52
10. List of tables	54

1. Introduction

1.1 Leishmaniasis

Leishmaniasis is a vector-borne infection caused by obligate intracellular *Leishmania* spp. and transmitted through the bite of female sand flies. Around 70 animal species, including humans, act as hosts of *Leishmania* parasites (World Health Organization (WHO)). Based on the World Health Organization (WHO) data, this infection is one of the seven most preeminent tropical diseases and a dominant health problem (Torres-Guerrero et al. 2017). Factors that contribute to the distribution of leishmaniasis are climate crisis, migration of population, long-distance tourism, trade and expansion of sand flies due to natural and human elements, such as deforestation, global warming and urbanization. Despite this, it is not given proper attention since it is most common in regions with low-income economies and limitations in the health care system (Kobets et al. 2012).

The type of pathology depends on the species of *Leishmania*, the genotype and nutritional status of the host, the transmitting vector and environmental and social factors (Kobets et al. 2012).

Leishmaniasis includes asymptomatic infections and three main clinical syndromes; in the dermis, parasites cause the cutaneous form of the disease; in the mucosa, they cause mucocutaneous leishmaniasis and the metastatic spread of infection to the spleen and liver leads to visceral leishmaniasis (also known as kala-azar or black fever). Parasites can also enter other organs, such as lymph nodes, bone marrow and lungs, and in rare cases they can even reach the brain. Cutaneous leishmaniasis is one of the top 10 diseases among tourists returning from tropical countries with skin problems (Kobets et al. 2012).

1.1.1 Epidemiology

Leishmaniasis is found in 89 countries. It is endemic in Asia, Africa, South and North America and the Mediterranean region. An estimated 1.5 to 2 million new cases occur each year and it causes 70,000 deaths per year (Torres-Guerrero et al. 2017). Based on geographical distribution, the disease is divided into Old World and New World leishmaniasis (Kobets et al. 2012).

Visceral leishmaniasis is prevalent in more than 60 countries, though 90% of the cases occur in six countries only: India, Bangladesh, Nepal, Brazil, Ethiopia and Sudan. The visceral form of the disease is caused primarily by *L. dovani* in India, Asia and Africa; *L. infantum* in the Mediterranean bases, and *L. chagasi* in South America. In Mediterranean countries, South America and Transcaucasia the disease is zoonotic and affects largely infants and young children. Stray and family dogs are the main host for the infection in these areas. In the

Indian subcontinent and Africa, visceral leishmaniasis is anthroponotic and can affect both adults and children (Kobets et al. 2012).

Table 1. The vector, disease and origin of different *Leishmania* species (Sunter and Gull 2017).

Species	Sand fly vector	Disease	Old world or new world
<i>L. major</i>	<i>Phlebotomus dubscqi</i> <i>Phlebotomus papatasi</i> <i>Phlebotomus Salehi</i>	cutaneous	old world
<i>L. mexicana</i>	<i>Lutzomyia olmeca</i>	cutaneous	new world
<i>L. braziliensis</i>	<i>Lutzomyia wellcomet</i> <i>Lutzomyia complexus</i> <i>Lutzomyia carrerai</i>	mucocutaneous	new world
<i>L. dovani</i>	<i>Phlebotomus argentipes</i> <i>Phlebotomus orientalis</i> <i>Phlebotomus martini</i>	visceral	old world
<i>L. infantum</i>	<i>Phlebotomus ariasi</i> <i>Phlebotomus perniciosus</i> <i>Lutzomyia longipalpis</i>	Visceral	new and old world

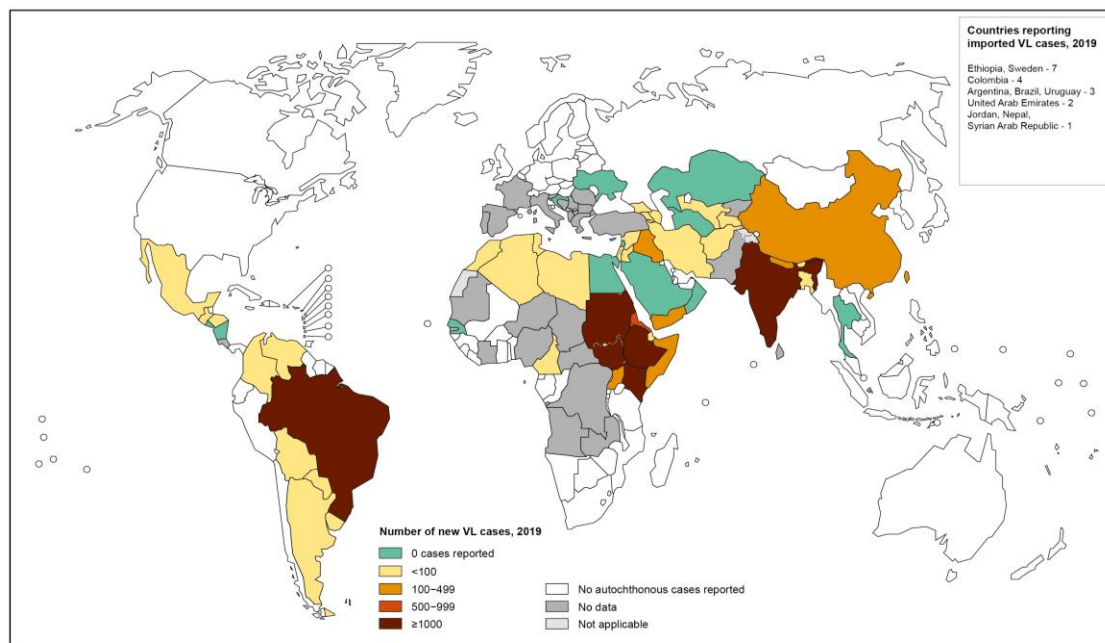


Figure 1. Status of endemicity of visceral leishmaniasis worldwide. Modified after (World Health Organization, 2019).

Cutaneous leishmaniasis is endemic in more than 70 countries. Afghanistan, Syria and Brazil are the main centers. The cutaneous form of the disease is triggered mainly by *L. tropica* and

L. major in the Old World, and by *L. braziliensis*, *L. Guyaneis*, *L. panemensis*, *L. mexicana*, *L. amazonensis* and *L. venezuelensis* in the New World. Mucosal leishmaniasis occurs in a small number of patients with New World cutaneous leishmaniasis, however, its course is chronic and can be life-threatening (Kobets et al. 2012).

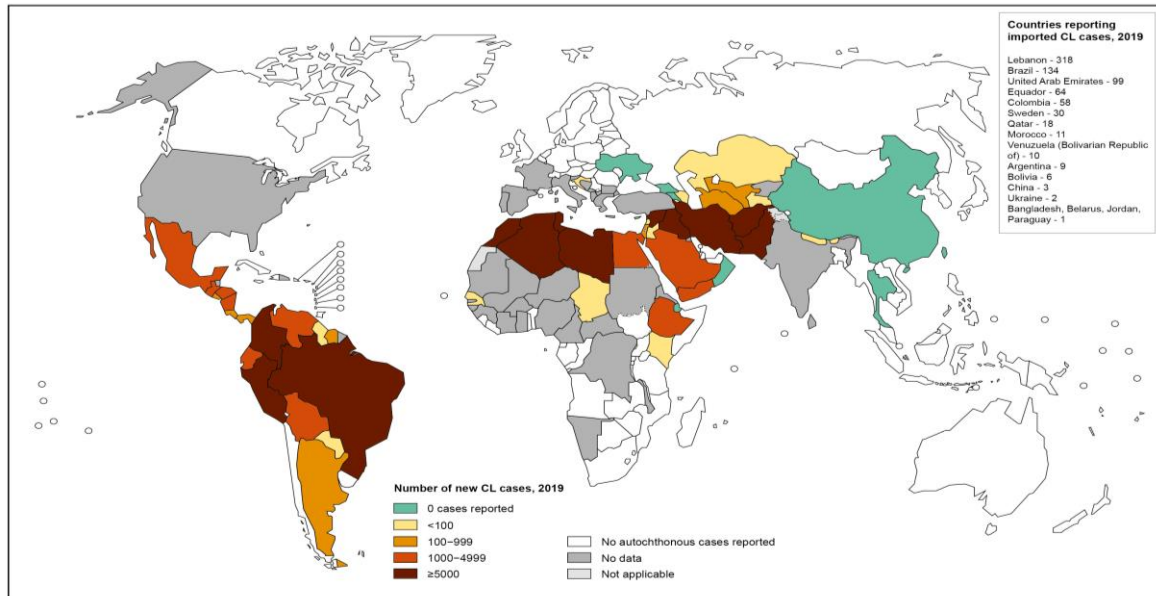


Figure 2. Status of endemicity of visceral leishmaniasis worldwide. Modified after (World Health Organization, 2019).

1.2 *Leishmania*

Leishmania have a digenetic life cycle, alternating between a vertebrate reservoir and an arthropod vector. In hosts and vectors, *Leishmania* cells have different cellular structure and developmental forms. The two major cell morphologies are promastigotes and amastigotes. Promastigotes are found in the sand fly and the amastigotes in mammalian hosts. Although both forms have a similar basic structure with the kinetoplast found in the anterior of the nucleus and a flagellum, they are very easy to differentiate from one another. Amastigotes are small spheric and immobile with a short flagellum, which acts as a sensor. On the other hand, promastigotes have an elongated structure, capable of movement due to the long flagellum (Sunter and Gull 2017).

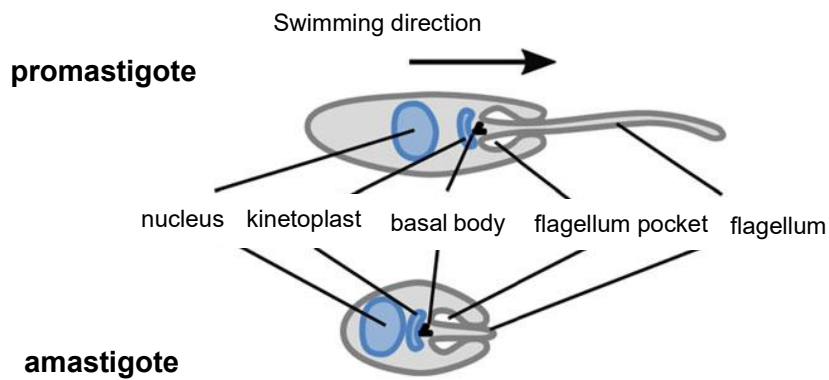


Figure 3. Morphological structures of a promastigote and an amastigote (Sunter and Gull 2017).

1.2.1 Life cycle of *Leishmania*

Leishmania cyclic promastigote cells of infected female sand flies enter the host through the site of the bite when the arthropod takes a blood meal. In the mammalian host organism neutrophils, monocytes and macrophages, dendritic cells, immature myeloid precursor cells, hepatocytes and fibroblast are infected by the parasite, but macrophages are mainly the resident cells of this pathogen. The invasion of macrophages can occur in the site of the bite or far away from it. Once the pathogen is engulfed the promastigote converts into the spherical amastigote. The differentiation occurs in the parasitophorus vacuole (PV) of macrophages and depends on the increase of temperature and presence of ferrous iron and the dropping of pH. The vacuole type can vary in different species of *Leishmania*. It is hypothesized that the flagellum can sense if the host cell is 'healthy' and the parasite can enter the cell cycle or if the cell is damaged and about to lyse and free the parasite into a new milieu (Sunter and Gull 2017).

The amastigotes develop into the promastigote form after the being ingested by the sand fly and freed from the immune cells of the host. The development can be triggered by a mixture of factors, such as the change in temperature or pH (Sunter and Gull 2017).

Apart from the two main parasite cell structures (amastigote and promastigote) there are other developmental forms in the sand fly such as: procyclic, nectomonad, leptomonad and metacyclic promastigotes. The procyclic structure has a cell body longer than the flagellum and it can be observed within the blood meal; the nectomonad form occurs in midgut and then it moves in the direction of the foregut, where it differentiates in leptomonad promastigotes. The leptomonad has a cell body length shorter than the flagellum and can either transform into the dominant form, metacyclic promastigotes, or haptomonad promastigotes. The metacyclic structure is the one that can infect the mammalian host cells (Sunter and Gull 2017). New findings have shown that metacyclic promastigotes can de-differentiate in the sand fly to boost population expansion of parasites in a second blood meal. This leads to a larger potential to spread the disease than after a first blood meal

(Bates 2018). The role of the haptomonad cell is unclear, but as it is rarely seen in cell cycle, it can be linked to the stomodeal valve of the sand fly and free to divide slowly (Sunter and Gull 2017).

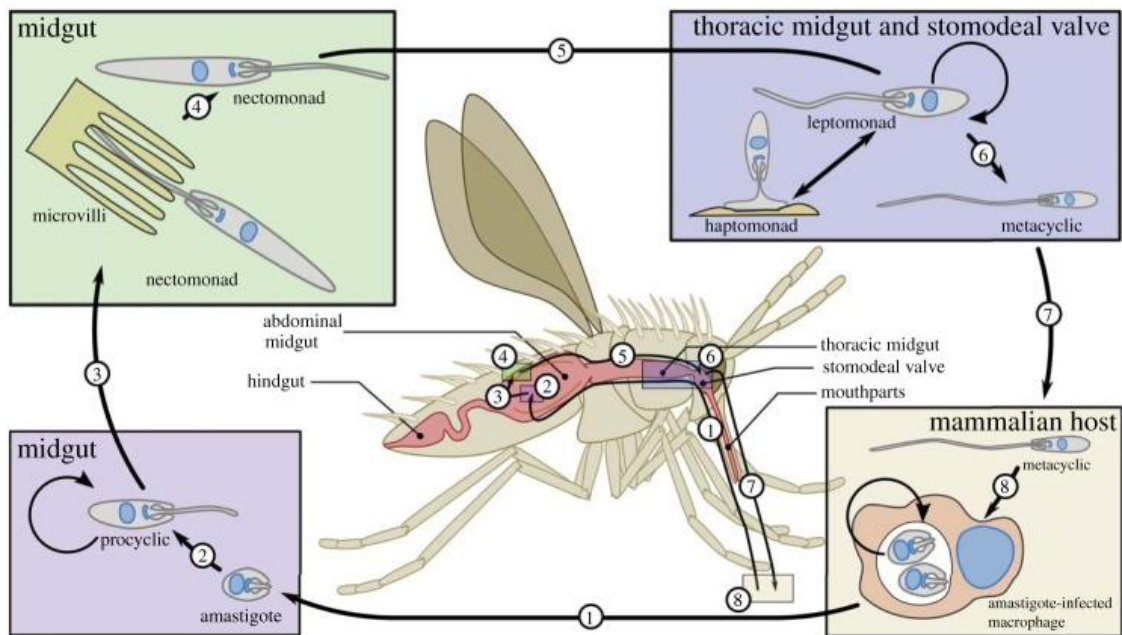


Figure 4. The life cycle of *Leishmania*. A sand fly takes blood from an ill host and ingests the amastigote structures inside macrophages. When they arrive in the midgut, amastigotes are differentiated into procyclic promastigotes, which later convert to nectomonad promastigotes that attach to microvilli in midgut. The nectomonads travel to thoracic midgut and stomodeal valve, where they develop into leptomonad promastigotes. The leptomonad promastigotes change into either haptomonad promastigotes that are found in stomodeal valve or into metacyclic promastigotes, which are ready to infect vertebrate hosts (Sunter and Gull 2017).

1.2.2 *Leishmania*-macrophage interaction

When the parasites enter the host organism, neutrophils and macrophages are employed in the site of the sand fly bite. At first, the promastigotes largely enter neutrophils, but they cannot differentiate into amastigotes inside of them. This leads to neutrophil apoptosis and the infected cells can then transmit infection to macrophages (Podinovskaia and Descoteaux 2015). Based on the cell movement, it is likely that the first contact with macrophages occurs through the flagellum. *Leishmania* uptake depends on the receptor, lipid micro-domain-regulated and actin-mediated uptake. Inside the cell, the parasite adjusts its cell body toward the nucleus and the flagellum in the direction of the cell periphery. The formation of PVs follows the union and fission of vesicles including endosomes and lysosomes. This process is highly species- and phase-reliant. The transformation from promastigotes to amastigotes is followed by a decline in growth rate and the production of a distinct metabolic state, such as a drop in uptake and consumption of glucose and amino acids, organic acid secretion and enhanced fatty acid beta-oxidation (Podinovskaia and Descoteaux 2015).

The growth process of *Leishmania* needs a supply of nutrients and extra membrane for phagosome enlargement. For the last requirement, the amastigote PVs interact with different secretory routes to transport ER elements to PVs. Amastigotes produce amino acid permeases and cysteine proteases to fulfill the need for amino acids. Another important part in growth play lipid bodies (LBs), which act as food source by providing triacylglycerol and sterol esters and provides proteins for PVs (Podinovskaia and Descoteaux 2015).

Leishmania perform a series of actions to weaken the macrophages defense. They manipulate specific cytokines in order to reduce infection-induced inflammation (a key point in macrophage activation) and promote a unique activation state in the macrophages that encourages their survival. On the one hand it interrupts apoptosis and on the other hand it uses the apoptotic host to spread the infection to other cells. *Leishmania* affects the host cell signaling by interfering the JAK-STAT pathway and hindering the antigen cross-presentation. This pathogen also avoids production of one of the key components providing protection of macrophages, the generation of reactive oxygen species (ROS) and reactive nitrogen intermediates. It does it by blocking NADPH oxidase construction and formation of ROS inside PVs. All the actions mentioned above are facilitated by *Leishmania's* intracellular survival factors, which differ based on the species and life cycle phase (Podinovskaia and Descoteaux 2015).

The most common surface glycolipid in promastigotes is lipophosphoglycan (LPG). It helps in the recruitment of phagosome maturation factors and in the fusion of it with the lysosome. LPG also protects the pathogenic cell by inhibiting NAPH oxidase formation (Podinovskaia and Descoteaux 2015). Zinc-dependent metalloprotease (GP63) is also commonly found in promastigotes and represents a metalloprotease that is glycosylphosphatidylinositol (GPI)-anchored. It is released into the macrophage by exosomes, as is a good portion of the other survival factors, to target host signaling and modify the cell to reduce TNF, IL -12, NO production and preservation of iron. Other important survival factors are inhibitors of serine peptidase (ISP), which deactivate host enzymes, such as neutrophil elastase, trypsin and chymotrypsin, to increase the parasite's chances of survival (Podinovskaia and Descoteaux 2015).

1.3 Treatments against leishmaniasis

WHO classifies leishmaniasis as a class I disease, that causes substantial morbidity and fatality rate. According to Centers for Disease Control and Prevention (CDC 2021) various laboratory methods are used to identify the parasite in the organism, such as analyzing of tissue specimens, ELISA methods and PCR by identifying the small subunit RNA genes. Even though the current treatment, chemotherapy, has shown some improvement n

managing the disease, it depends on management of drugs with high expenses, complicated path of administration and severe side effects that can trigger toxicity. A rise in resistant cases has also been reported due to treatments not being able to kill the parasite entirely from infected patients (Menezes et al. 2015). Therefore, it is challenging to design drugs that directly target the infected macrophages. Because of these problem the scientific and medical companies do not make a lot of efforts to find new treatment methods and possible drug targets, that not only are effective but also affordable for the population that it effects.

1.3.1 Vaccine candidates

There is currently no vaccine approved in humans for prevention of leishmaniasis. The selection of vaccine candidates is difficult because of the large number of antigens, different levels of effectiveness, and different animal models chosen. There have been first-generation vaccine candidates using killed pathogenic cells administered with or without adjuvants. The results of these trails have been unreliable due to application of variable factors like adjuvants and administration pathways. The use of genetically modified parasites or viruses expressing *Leishmania* genes encoding for recombinant proteins are bases for second-generation vaccines. Additional adjuvants can increase the potency of second-generation vaccines. Examples of peptide vaccines are GP63 or leishmanolysin, *Leishmania* activated C kinase (LACK) protein and hydrophilic acylated surface proteins (HASP) (Hossein and Moafi 2015). The low price, stability and standardized production makes the recombinant peptide vaccines more reliable compared to other candidates (Petitdidier et al. 2019). Naked DNA vaccines are known as third generation vaccines. They are safe compared to the other vaccines as they do not contain any pathogenic material. However, they have been proven to be inadequate in non-murine models (Hossein and Moafi 2015). Other options are leishmanization (live-inoculated *Leishmania*) and saliva vaccine with salivary molecules against leishmaniasis. The vaccines have been mainly tested in murine and/or canine models, but none of the clinical trials have shown effectivity in humans.

1.3.2 Pentavalent antimonials

The use of pentavalent antimonials, was a milestone in chemotherapy against leishmaniasis. Currently it is the most abundant drug treatment againts this parasite, even though it shows inconsistent effectivity (35-95 % depending on area) against visceral and cutaneous leishmaniasis (Menezes et al. 2015). It is administered through painful injections in intramuscular (IM), intravenous (IV) and intralymphatic (IL) areas, over a period between 28 to 30 days. This drug is easily available and found in low cost, however, it can cause severe side effects: vomiting, nausea, anorexia, myalgia, headache, lethargy and seldom fatal cardiac arrhythmia due to buildup in tissue and toxicity. Attempts have been made to improve

the lengthy treatment, and to reduce the number of resistance development and toxicity issues. But they have not been successful (Menezes et al. 2015).

There are two important antimonial compounds, complexes of Sb^V with N-methyl-D-glucamine and sodium gluconate. Their mechanism of action is yet still unclear. It is hypothesized that they can either work as a prodrug and when they reach their target they transform in a more toxic form or they are active drugs that demonstrate an intrinsic antileishmanial activity (Palma et al. 2018).

1.3.3 Amphotericin B

Amphotericin B (AmB) is a polyene antibiotic and is primarily used in leishmaniasis treatment. Unfortunately, it displays severe nephrotoxicity, infusion-related reactions and hypokalemia. Patients, who are treated with AmB need prolonged hospitalization, around 15 to 20 days. Its administration requires slow intravenous infusion and the taken dosage is limited. It can be either taken daily or infrequently to avoid toxicity (Menezes et al. 2015).

What makes this antibiotic useful in fighting leishmaniasis is its ability to bind to ergosterol. Ergosterol is the most abundant sterol in *Leishmania*. AmB uses ergosterol of *Leishmania* and macrophages to form transmembrane channels. The channels allow cations, water and glucose to pass and affect the enzymes found in the plasma membrane. It is this permeability effect in renal tubes of the host that leads to decreased pH and increased Ca²⁺ concentration, eventually regulated cell death and nephrotoxicity (Palma et al. 2018).

To reduce its side effects, new efficient formulations of AmB, such as a liposomes and lipid complex colloidal forms have been produced. The use of liposomal AmB lessens the side effects of the drug by encouraging superior tissue absorption and supporting drug penetration in macrophages. However, these substitutes are not affordable in developing countries and unstable in the extreme temperatures of the tropical and subtropical areas, where leishmaniasis is endemic (Menezes et al. 2015; Ortega et al. 2017).

1.3.4 Pentamidine

Pentamidine is an aromatic diamine used primarily as antifungal drug. It is not often used due to the rise of resistance cases because of decreased uptake followed by enhanced efflux of drugs. It is advised to be administered in combined curative protocols for better efficacy. In monotherapy it causes serious side effects: diabetes mellitus, hypoglycemia, myocarditis, hypotension and renal toxicity. There are reports that it has even led to death. It has restricted activity in different *Leishmania* species (Menezes et al. 2015). Its exact mechanism of action is not yet understood; however, it is reported that the drug enters inside *L. donovani* promastigote via arginine and polyamine transporters. Moreover, this drug gets stored in mitochondria and increases efficacy of respiratory chain complex II inhibitors suggesting its leishmanicidal activities due to reduced mitochondrial membrane potential

(Singh et al. 2012). In vitro studies of pentamidine analogs have shown potential as new treatments with reduced toxicity (Singh et al. 2012; Menezes et al. 2015; Bell et al. 1990).

1.3.5 Paromomycin

Paromomycin, an aminoglycosidic antibiotic, is an antifungal alternative drug also used for treatment of leishmaniasis. It is administered differently varying on the clinical manifestation of the disease. In visceral leishmaniasis IM administration is commonly used and for cutaneous leishmaniasis there are topical formulations. Its mode of action is unclear. Cationic paromomycin attaches to the negatively charged leishmanial glycocalyx indicating mitochondria as a primary target. Paromomycin hinders translocation and recycling of ribosomal subunits and consequently protein synthesis (Singh et al. 2012; Menezes et al. 2015). Its effectiveness varies in different regions and its administration is followed by toxicity in liver, ear and kidneys. Paromomycin is the cheapest drug used against leishmaniasis (Singh et al. 2012; Menezes et al. 2015).

1.3.6 Miltefosine

Miltefosine is an alkyl-phosphocholine analogue, that shows most promising results in chemotherapy. In contrast to other drugs, it is administered orally. However, it gives rise to occurrence of resistant cases because of its long terminal residence time. The median long half-life of miltefosine, approximately 152 hours, could trigger the progress of clinical resistance. It is not recommended in pregnant women as it can induce teratogenesis. The exact mechanism is not yet known, but it has been found that it triggers apoptosis like processes in *L. donovani*. Miltefosine decreases the amount of lipids in promastigote membranes, which leads to decline in parasite proliferation (Singh et al. 2012; Menezes et al. 2015). Other side effects include vomiting, diarrhea, toxicity in liver and kidneys. Treatment of leishmaniasis with miltefosine is expensive (Singh et al. 2012; Menezes et al. 2015).

1.3.7 Combination therapy

Combination therapy protocols have been set up to achieve a more successful treatment of leishmaniasis. They have greatly reduced individual doses, cost and period of treatment. Other advantages are expected from these protocols, such as a lower toxicity, hindrance of resistance development and boost of activity (Menezes et al. 2015; Scariot et al. 2017).

A potential combination is miltefosine with AmB or paromomycin that could be helpful to treat antimonial-resistant visceral leishmaniasis. Other studies have been conducted with combining drugs: liposomal formulations of AmB, miltefosine and paromomycin. The combination therapy was compared to the monotherapy of each drug. Although it showed no better effectiveness, the period of the treatment and the side effects were reduced (Menezes et al. 2015).

1.4 Endoperoxides

Peroxides are chemical compounds containing the bivalent oxygen bridge (-O-O-). They are represented as R-O-O-R. The most familiar of them is hydrogen peroxide (H₂O₂). Peroxides are partially instable and have oxidative properties. Inorganic peroxides react with organic compounds to deliver organic peroxides and hydroperoxide products. Organic peroxides are derivatives of hydrogen peroxide where one or both hydrogen atoms are replaced by carbon atoms. The most common structural representation is R-O-O-H (alkyl or aryl hydroperoxides) or R-O-O-R₁ (dialkyl peroxides) (Clark 2000). On the other hand, endoperoxides (EP) contain their O-O bond between two carbons in a cyclic carbon ring. EPs are created by Diels-Alder addition of singlet oxygen to 1,3-dienes (Jefford 1996). By the process of cycloreversion they can release the singlet oxygen again (Fudickar and Linker 2018). EPs are also found temporarily in the human body as intermediates of prostaglandin production, such as PGH₂ generated by cyclooxygenase (COX) enzymes (Ricciotti and FitzGerald 2011; Zurier 2017).

A group of EPs, artemisinin's, are employed as antimalaria drugs. They are effective against *Plasmodium* species in humans by reducing the parasite number already at nanomolar concentrations. Their mechanism of action is not fully elucidated yet. However, it is assumed that its action starts with the breaking of the O-O bridge by heme freed by *Plasmodium* hemoglobin digestion in erythrocytes. This results in the release carbon-centered radicals and alkylating intermediates, that damage and decrease proteins associated with malaria parasite survival (Tran et al. 2018).

Artesunate, a semisynthetic derivative of artemisinin, is an even more efficient antimalaria drug, since it is water-soluble and can be taken orally, besides IV and IM administration (Tran et al. 2018).

As a consequence of these findings, other newly synthesized EPs, such as anthracene endoperoxides (AcEPs) should be studied for their antileishmanial potential in suitable testing conditions.

1.4.1 Effects of endoperoxides in *Leishmania*

Oxidative stress is a threat for both mammalian cells and eukaryotic microorganism. Large amounts of ROS can cause pathologies. Even though antioxidant enzymes and chemicals of these organisms can differ, the basic principles are similar to prevent extreme ROS formation and damage. Due to antioxidant defense, pharmacological drugs that rely on peroxides are not the primary choice against intracellular parasites since H₂O₂ and lipid hydroperoxides are efficiently detoxified in the macrophage host cells. However, the use of EPs, such as artemisinin, against malaria has been established. They are less targeted by the host cell defense. Even though *Plasmodia* and *Leishmania* species have many different

characteristics, reliance on iron supply from the host cell is a common feature. Pathogens become vulnerable to EPs when oxidative stress is triggered by free iron in labile iron pool (LIP) (Geroldinger et al. 2017).

Previous studies have shown that the EP ascaridole (Asc) is a potential antileishmanial drug (Monzote et al. 2014; Geroldinger et al. 2017). Thereafter, it was reasonable to investigate EPs with different structures as antileishmanial drugs. A new synthetic group of compounds are the anthracene endoperoxides (AcEPs), derived from the reaction of substituted anthracenes with singlet oxygen by cycloaddition. Some of the compounds were studied *in vitro* using *L. tarentolae*, *L. donovani* and a mouse macrophage cell line. The gathered data demonstrated that certain AcEPs were killing the *Leishmania tarentolae* promastigotes (LtP) more effectively than J774 macrophages (Geroldinger et al. 2018).

1.5 Test systems

Attempts for the advancement of new therapeutics, necessary for the control of leishmaniasis depend on screening of potentially effective compounds in pathogen growth/multiplication assays, both *in vitro* and *in vivo* (Gupta 2011).

1.5.1 *In vitro*

The advantages of *in vitro* drug testing are that the parasites from a few animals are sufficient to test many compounds, the requirement of test compound is very minute, and the turnover of screening results are fast; and the results are reliable (Gupta 2011).

The promastigotes grown in simple media have been used as test parasites to screen potential antileishmanial agents. This system is widely popular due to its simplicity. The simplest model to be utilized is the one in which the promastigotes multiply in cell free media. The technique is simple and easily applicable. Nevertheless, the metabolism and ecology of promastigotes vary so widely from those of intracellular amastigotes (target form) that screening data acquired from *in vitro* test with promastigotes have limitations. Another disadvantage of this system is lower temperature (24 °C) at which the culture grows, as opposed to the *in vivo* temperature of 37 °C. The problem is that promastigotes in culture at 37 °C will survive but not multiply (Gupta 2011).

Screening against axenic amastigotes has some advantages; the test is directed against the relevant stage of parasite. Screening with axenic amastigotes from clinical isolates is not possible because they need time to get adapted in the cultures. Furthermore, axenic amastigotes have different metabolic processes than intracellular amastigotes (Gupta 2011).

Intracellular amastigotes are the most widely used system for testing drugs against *Leishmania* species. The host cells can be either be murine peritoneal macrophages or

human-monocyte transformed macrophages (THP-1, U937, and HL-60). The rate of amastigote division in host cells and drug activity can be easily measured, in bone-marrow-derived macrophages. They imitate the environment met by the target cell. However, the slow rate of division of *L. donovani* and *L. infantum* amastigotes in this model is a drawback. Testing with intracellular amastigotes is labour intensive, results are variable and it is difficult to screen a number of drugs simultaneously (Gupta 2011).

Nevertheless, the diversity of *Leishmania* species, its clinical manifestation and the intracellular location of this pathogen makes it difficult for research. Furthermore, most of *Leishmania* species belong to biosafety class 2 (*L. donovani*) or even higher. Therefore, LtP are used in the first stages of antileishmanial drug analysis. In this study, LtP was used. *L. tarantolae* (biosafety class 1) is a lizard pathogen and nonpathogenic to human. It belongs to the subgenus *Sauroleishmania* and is the best studied non-pathogenic species of this *Leishmania* subgenus. It represents a safe model, are easy to cultivate and its biology is comparable to pathogenic *Leishmania* (Cao et al. 2019; Klatt et al. 2019).

Macrophage-like cells lines from different origins are responsive to *Leishmania* infection (Santarém et al. 2019). There are a number of cell lines suitable as macrophage models, such as the human THP-1 and U937 and the murine RAW264.7 and J774 cell lines (Madhvi et al. 2019). THP-1 cell line is generally used as it can be differentiated with phorbol-12myristate-13-acetate (PMA) into macrophages that are susceptible to *Leishmania* infection (Santarém et al. 2019). The model used in our study was J774A.1 (mouse, ATCC, TIB-67™), an immortalized murine-macrophage like cell line.

1.5.2. In vivo

Popular in vivo models used for the study of *Leishmania* infections are rodents, including inbred and outbred mouse strains and hamsters. These animal models have given vital information on the immunopathology of the disease and host-pathogen relationships. However, because they all derive from a relatively small pool of descendants, their genetic background is rather restricted. Laboratory studies using natural hosts allow a better grasp of the varying aspects of infection, especially concerning the ability to keep the infection and expand parasite populations in a given environment. However, difficulties in containing wild animals in captivity have made it hard to follow up the infection wild reservoirs by *Leishmania* species in experimental settings (Loría-Cervera and Andrade-Narváez 2014).

Dogs have an important role as domestic host in *Leishmania* parasite. This makes them a preferred model for better insight of their position in *Leishmania* transmission and for testing drug usefulness (Loría-Cervera and Andrade-Narváez 2014).

Moreover, non-human primates would be the most suitable model because of their resemblances to humans in anatomy, immunology, and physiology. Still, they are expensive laboratory animals that are difficult to acquire and to manage (Loría-Cervera and Andrade-Narváez 2014).

1.6 Viability assays

A viability assay examines the effects of a substance in different concentrations on the metabolic or morphological appearance of specific cell types. Viability tests can be performed in all cellular models relevant for the *Leishmania*/macrophage system. Based on the resulting viabilities at different concentrations a concentration-viability curve can be constructed. From these curves the half maximal inhibitory concentrations (IC_{50}) can be determined, which is the concentration of a compound which kills 50% of the respective cells. The lower the value, the more effective is the drug. Antileishmanial drugs need to have a low IC_{50} in *Leishmania* viability assays and high IC_{50} values in macrophages assays (that means to not affect the host cells). Those compounds are possible candidates as antileishmanial drugs. Apart from conventional viability methods that aim to test the individual effect of a single compound, combination viability assays study the simultaneous interaction of two or more drugs on the target cells. This is important, since it has been shown that combinatorial therapies can increase the effectivity of drugs and reduce the treatment period. In a previous study (Zahid et al. 2019), combination assays were conducted with varying AmB concentrations at fixed and sub-optimal concentrations of other antileishmanial compounds, such as miltefosine and paromycin. Parasite viability in comparison to untreated controls was evaluated for individual drugs and their combinations. For each combination, the fractional inhibitory concentration index (FIC) was calculated with the equation:

$$FIC = \frac{IC_{50A,Combination}}{IC_{50A}} + \frac{C_{50B,Combination}}{IC_{50B}}$$

Equation 1. FIC is an index to measure synergy and antagonism. $IC_{50A,Combination}$ and $C_{50B,Combination}$ are the IC_{50} concentrations of the corresponding drugs in combination, and IC_{50A} and IC_{50B} are the IC_{50} values of the drugs when administered separately (Zahid et al. 2019).

An FIC index equal to 1 represented the additivity line, so FIC values above the error range of the additivity line corresponded to antagonistic effects between the drugs and FIC values below the additivity line error range pointed to synergistic outcomes (Zahid et al. 2019).

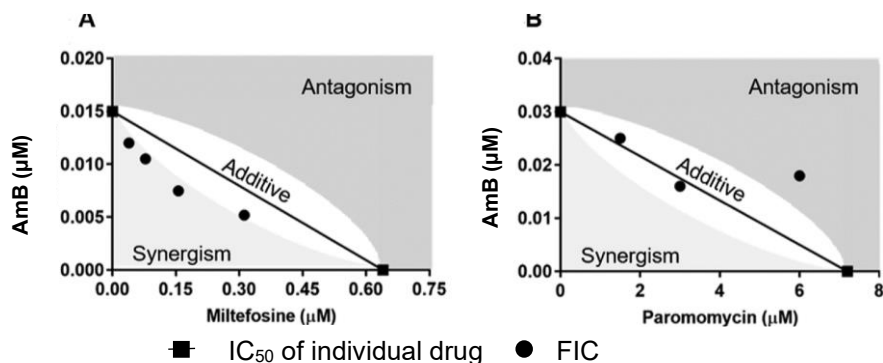


Figure 5. (A) AmB and miltefosine show mild synergetics effects, while (B) paromomycin with AmB showed additive interaction in low doses and antagonism in higher doses. (Zahid et al. 2019)

So far these combination assays are laborious, time consuming and difficult to use in large screening studies. Therefore, new combination methods have to be established and improved to get more precise results with less efforts and shorter time to screen more compound combinations.

1.7 Aims of the study

The aims of the current work were:

- i) A first major aim was to establish refined methods for viability testing as well as methods to testing the synergy of potential antileishmanial compounds.
- ii) A second major aim was to explore the antileishmanial activity of newly synthesized AcEP in comparison to their non-peroxidic anthracenes (Ac). This included the determination of the influence of these compounds on the viability of LtP and J774 cells. Furthermore, we tried to elucidate whether these compounds trigger superoxide radical formation in LtP as well as their reaction mechanism with iron and their thermal decomposition.

2. Materials and Methods

2.1 Chemicals

Chemicals that were used for sample preparation and maintenance work during this study are listed in Table 2.

Table 2. List of chemicals used for sample preparation and maintenance work.

Chemical	Supplier
Acetonitril (ACN)	Merck (Darmstadt, Germany)
Anthracene endoperoxides and analogues (AcEP, Ac)	Prof. T. Linker, Univ. Potsdam, Germany
Antimycin A (AA)	Sigma-Aldrich (St. Louis, Missouri, USA)
Brain Heart Infusion medium (BHI)	Sigma-Aldrich (St. Louis, Missouri, USA)
Hydroxyl-3-methoxycarbonyl-2,2,5,5-tetramethylpyrrolidine hydrochloride (CMH)	Noxygen (Elzach, Germany)
Deferoxamine (DFO)	Novartis (Basel, Switzerland)
Dulbecco's modified eagle's medium (DMEM)	Thermo Fisher Scientific (Waltham, MA, USA)
5,5-dimethyl-1-pyrroline N-oxide (DMPO)	Sigma-Aldrich (St. Louis, Missouri, USA)
Dimethyl sulfoxide (DMSO)	VWR (Radnor, Pennsylvania, USA)
Diethylenetriaminepentaacetic acid (DTPA)	Merck (Darmstadt, Germany)
Ethylenediaminetetraacetic acid (EDTA)	Merck (Darmstadt, Germany)
Fetal calf serum (FCS)	Bio & Sell (Nuernberg, Germany)
Hemin	Sigma-Aldrich (St. Louis, Missouri, USA)
K ₂ HPO ₄	Merck (Darmstadt, Germany)
KH ₂ PO ₄	Merck (Darmstadt, Germany)
Miltefosine	Acros Organics (New Jersey, USA)
Na ₂ HPO ₄	Merck (Darmstadt, Germany)
NaCl	Merck (Darmstadt, Germany)
Penicillin-streptomycin solution	VWR (Radnor, Pennsylvania, USA)
Pentamidine (Pen)	Sigma-Aldrich (St. Louis, Missouri, USA)
Resazurin	Sigma-Aldrich (St. Louis, Missouri, USA)
Xylenol orange (XO)	Merck (Darmstadt, Germany)
Yeast extract (YE)	Amresco (Solon, Ohio, USA)

2.2 Endoperoxides and analogues

The structures of the AcEPs, their corresponding non-endoperoxides and other substances that have been used in different methods during this work are shown in Figure 6. The IUPAC names of each of the AcEPs and their Ac are listed in Table 3.

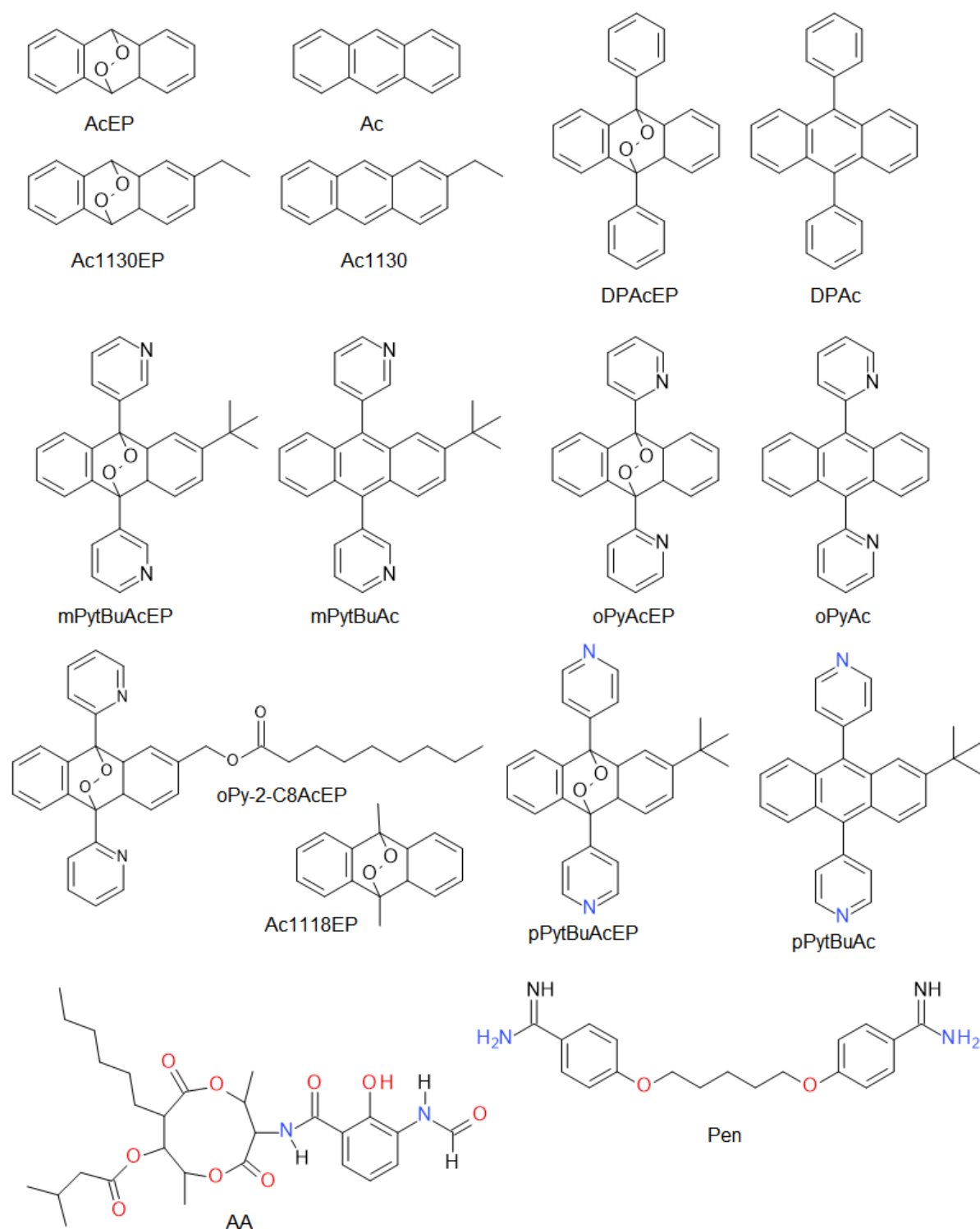


Figure 6. Structures and abbreviations of AcEPs, their corresponding Ac, Pen (control substance) and AA.

Table 3. IUPAC names of AcEPs and their corresponding non-endoperoxides used in this work.

Abbreviation	IUPAC Name
Ac	Anthracene
AcEP	15,16-dioxatetracyclo[6.6.2.02,7.09,14]hexadeca-2(7),3,5,10,12-pentaene
Ac1118	1,8-dimethyl-15,16-dioxatetracyclo[6.6.2.02,7.09,14]hexadeca-2(7),3,5,10,12-pentaene
Ac1130	2-ethylanthracene
Ac1130EP	11-ethyl-15,16-dioxatetracyclo[6.6.2.02,7.09,14]hexadeca-2(7),3,5,10,12-pentaene
DPAc	9,10-diphenylanthracene
DPAcEP	1,8-diphenyl-15,16-dioxatetracyclo[6.6.2.02,7.09,14]hexadeca-2(7),3,5,10,12-pentaene
mPyBuAc	3-[2-tert-butyl-10-(3-pyridyl)-9-anthryl]pyridine
mPyBuAcEP	3-[11-tert-butyl-8-(3-pyridyl)-15,16-dioxatetracyclo[6.6.2.02,7.09,14]hexadeca-2(7),3,5,10,12-pentaen-1-yl]pyridine
oPyAc	2-[10-(2-pyridyl)-9-anthryl]pyridine
oPyAcEP	2-[8-(2-pyridyl)-15,16-dioxatetracyclo[6.6.2.02,7.09,14]hexadeca-2(7),3,5,10,12-pentaen-1-yl]pyridine
pPyBuAc	4-[2-tert-butyl-10-(4-pyridyl)-9-anthryl]pyridine
pPyBuAcEP	4-[11-tert-butyl-8-(4-pyridyl)-15,16-dioxatetracyclo[6.6.2.02,7.09,14]hexadeca-2(7),3,5,10,12-pentaen-1-yl]pyridine

2.3 Cell culture

2.3.1 LtP cell culture

Leishmania tarentolae promastigotes (LtP) (strain P10 from Jena Bioscience, Germany) were employed as biological system in tests performed in this work. Brain heart infusion (BHI) medium (37 g/L, pH 7.4) accompanied with 5 mg/L hemin and 25.000 U/L penicillin – 25 mg/L streptomycin (against bacterial contamination) in 50 mL TubeSpin bioreactors (VWR) was used to cultivate LtP. The parasites were grown in an incubator (Cytoperm, Heraeus Instruments, Hanau, Germany) at 26.5 °C on a shaker (0.05 s⁻¹). The passage of cell culture was performed three times a week and the new cell culture had a density of 18 * 10⁶ LtP/mL or 36 * 10⁶ LtP/mL. To find the cell count, the optical density (OD) of an 1:8 diluted aliquot was measured with a photometer (U-1100, Hitachi Ltd, Tokyo, Japan) at 600 nm. The formula used for calculating the number of cells found in 1 mL is (Fritsche 2008):

$$x \cdot 10^6 \text{ cells /mL} = \text{OD}_{600} \cdot 0.969 \cdot 124$$

0.969 - conversion factor [g/L] dry weight

124 - 1 g dry weight/L correspond to 124 * 10⁶ cells/mL

LtP were used for experiments, a day after passage.

2.3.2 J774 macrophage cell culture

The other biological system in this work was a murine macrophage cell line J774A.1 (mouse, ATCC, TIB-67™). J774 was cultivated in DMEM (high glucose, 1.5 g/L NaHCO₃) with 25,000 IU/L penicillin, 25 mg/L streptomycin, and 10 % FCS (heat-inactivated) in 50 mL TubeSpin bioreactors. The cell line was incubated on a roller culture apparatus (5 rpm) at 37 °C and 5 % CO₂. The J774 macrophages were counted by taking 8 pictures of the cells in a Thoma chamber with a camera/microscope combination at 40x magnification and subsequent counting by the cell image analysis (CIA) software of own design. According to the determined cell concentration, the culture was passaged three times a week adjusting the new culture on Monday and Wednesday to a density of 0.2*10⁶ cells/mL and on Friday to a density of 0.1*10⁶ cells/mL.

2.4 Viability assays

2.4.1 Viability assay for LtP

The viability assays were carried out in 96-well non-treated cell culture plates (Eppendorf, Art. nr. 30730011). YEM medium (20.7 g/L yeast extract powder, 1.2 g/L K₂HPO₄, 0.2 g/L KH₂PO₄, 2.9 g/L glucose, pH 7.4) and PBS (136 mM NaCl, 1.15 mM KH₂PO₄, 14 mM

Na_2HPO_4 , and 2.7 mM KCl, pH 7.4) with 25,000 U/L penicillin, 25 mg/L streptomycin, and 6 μM hemin was prepared with 2×10^6 LtP/mL, if required.

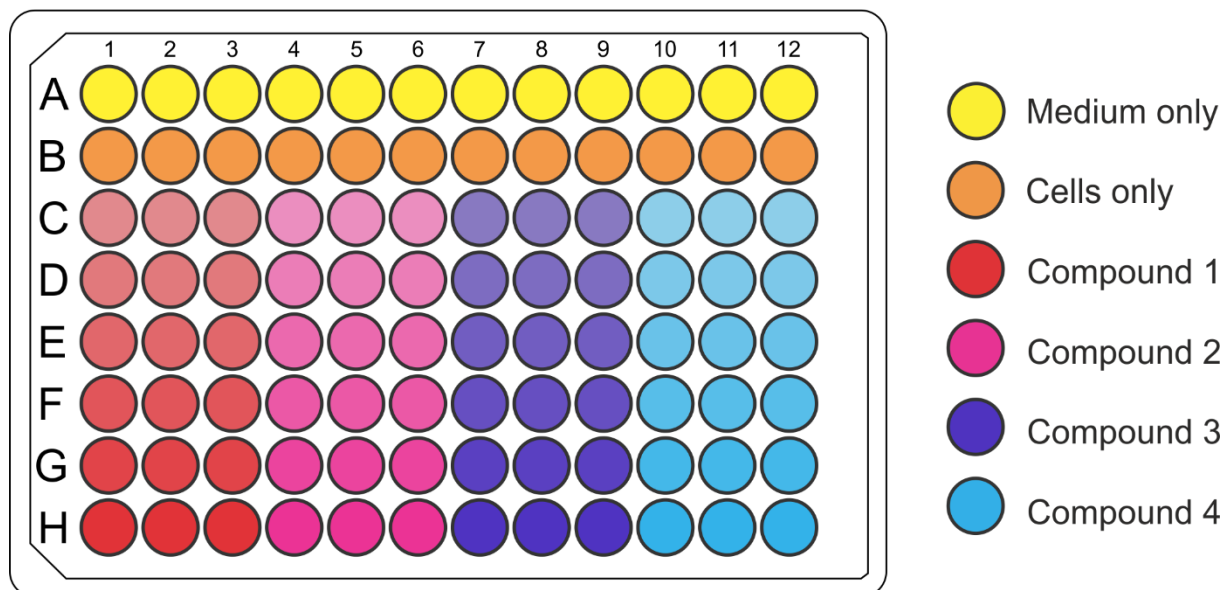


Figure 7. Vertical serial dilution viability assay. Row A was the negative control and the positive control was row B. Rows C-H contained mixtures of YEM/PBS medium with cells and compounds tested in triplicates. The highest compound concentration was in row H and row C had the lowest concentration.

In the vertical viability assay (Figure 7), row A served as a negative control (0 % viability), with 200 μL YEM/PBS medium per well. Aliquots of 200 μL of the YEM/PBS with cells were distributed in the remaining wells (row B-H) in the non-treated cell culture plate. Row B acted as a positive control (100 % viability). In row H, wells were additionally filled with extra medium for the serial dilution step. Aliquots of compound stocks were added at different initial concentration depending on the substance to row H and then 1:3 vertical serial dilution was carried out from row H to C disposing the final transfer volume. In each plate, four compounds were tested in triplicates. After this step 8 ml PBS (1 ml at each outer edge and 4 ml in the middle) were placed between the wells. The plates were incubated for 48 h at 26.5 $^{\circ}\text{C}$. After incubation, 50 μL of resazurin solution in PBS were added in each well (final concentration 20 μM). Following another 4 h incubation under the same conditions, the fluorescence was measured at 590 nm emission with 560 nm excitation using a plate reader (Perkin Elmer Enspire, Germany). A four-parameter logistic model was used to calculate the IC50 values using a custom designed Excel worksheet with Python support.

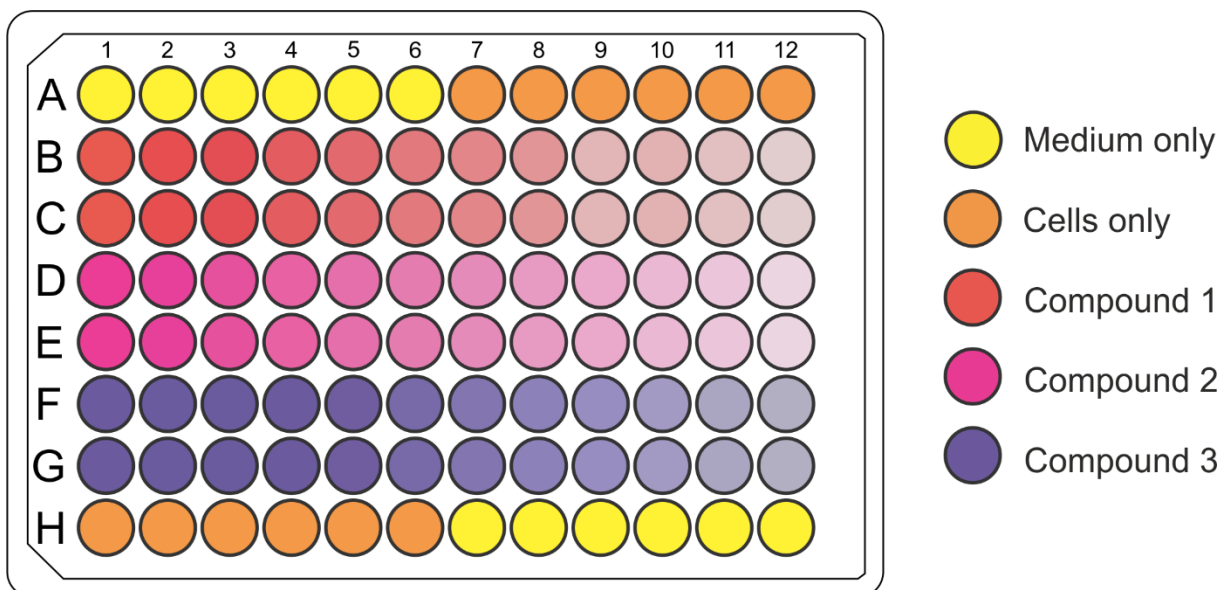


Figure 8. Horizontal serial dilution viability assay. Row A, column 1-6 and row H, column 7-12 were the negative control and the wells of row A, column 7-12 and row H, column 1-6 served as positive control. Column 1, rows B-G contained the YEM/PBS medium with cell mixtures and compounds which were tested in duplicates. Column 1 had the highest compound concentration, while column 12 the lowest.

The horizontal viability test with horizontal serial dilution was established in this work (Figure 8). For the viability assays of single compounds, 200 μL of YEM/PBS (1:1) medium were added in each well in negative control (0 % viability) row A, column 1-6 and row H, column 7-12. The wells of row A, column 7-12 and row H, column 1-6 served as positive control (100 % viability). In each well 200 μL of the mixture of the cells with YEM/PBS medium were added. In the remaining wells (row B-G) 100 μL YEM/PBS medium were pipetted. In column 1, wells were additionally filled with extra medium for the serial dilution step. Aliquots of compound stocks were added at different initial concentrations depending on the substances in column 1. Then 1:2 horizontal serial dilution was conducted, starting from column 1 to column 12 disposing the final transfer volume. Then 100 μL mixture of LtP with YEM/PBS medium were added in rows B-G. On each plate three compounds were tested in duplicates. After this step 8 ml PBS (1 ml at each outer edge and 4 ml in the middle) were placed between the wells. The plates were incubated for 48 h at 26.5 $^{\circ}\text{C}$. Then, 50 μL of resazurin solution in PBS were added in each well (final concentration 20 μM). After another 4 h incubation under the same conditions, the fluorescence was measured at 590 nm emission with 560 nm excitation using a plate reader (Perkin Elmer Enspire, Germany). A four-parameter logistic model was used to calculate the IC₅₀ values using a custom designed Excel worksheet with Python support.

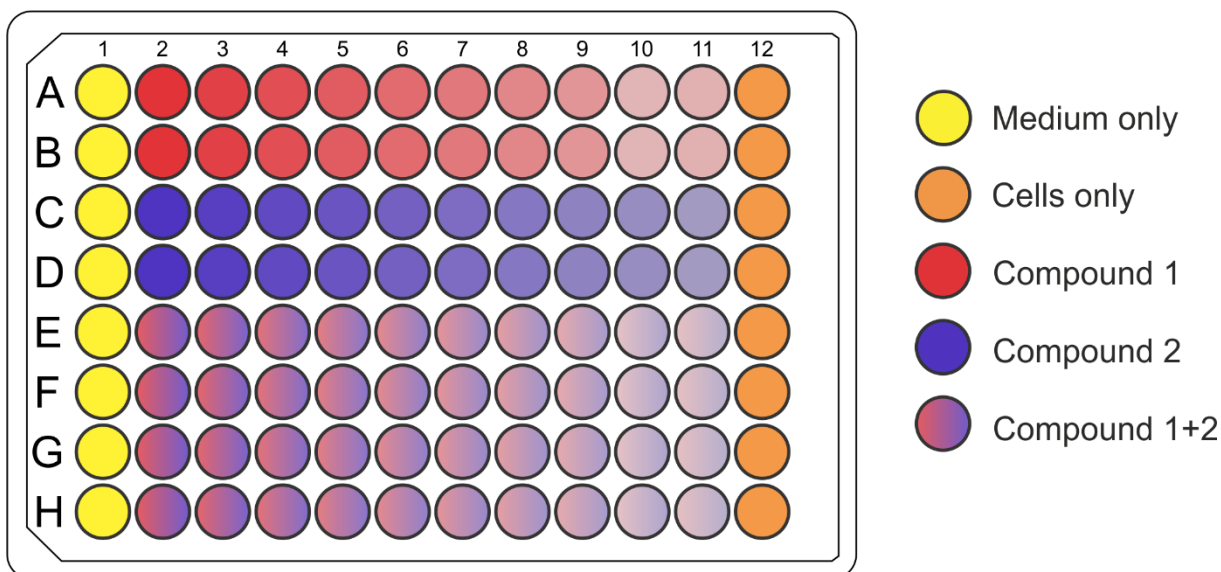


Figure 9. Combination viability assay. Column 1 contained only YEM/PBS medium (negative control). Column 12 acted as positive control containing medium with cells. In column 2, rows A-D contained the compounds separately in duplicates and rows E-H had a mixture of both compounds. Column 2 had the highest concentration of compounds, while column 11 contained the lowest.

In the combination viability assay, column 1 acted as negative control with 200 μL of YEM/PBS medium in each well (0 % viability). The positive control well, column 12, had 200 μL of LtP with YEM/PBS medium mixture. In columns 1-11, 100 μL YEM/PBS medium were added and then in column 2 extra medium was pipetted for the serial dilution. Aliquots of two compounds with different initial concentration were used to test the synergy in column 2. In rows A-D, column 2 the compounds were added separately in duplicates. Wells in rows D-H, column 2 were filled with a mixture of both compounds. Then 1:2 horizontal serial dilution was conducted, starting from column 2 to column 11 and the final transfer volume was disposed. After this step 8 ml PBS (1 ml at each outer edge and 4 ml in the middle) were placed between the wells. The incubation period and conditions were the same as that for assays of single compounds. After 48 h, 50 μL of resazurin solution in PBS were added in each well, giving a final concentration of 20 μM . After another 4 h incubation the fluorescence was measured as described above. The viability of LtP in the combination method was calculated by using a custom designed Excel worksheet with Python support. At first IC_{50} values of each single compound were calculated and the FIC (see equation 1) was determined. FIC values below 0.5 are considered as synergism.

2.4.2 Viability assay for J774 macrophages

The viability assays for J774 macrophages were carried out in 96-well cell culture treated plates (Eppendorf, Art.nr. 30730119). A mixture of DMEM containing 25,000 U/L penicillin, 25 mg/L streptomycin, and 10 % FCS with 1×10^5 J774/ml was prepared. Then 200 μL of this mixture were added in rows B-H and 8 ml PBS (1 ml at each outer edge and 4 ml in the middle) were placed between the wells. After this step plates were incubated for 24 h at 37

°C and 5 % CO₂ to allow attachment. The next day, the medium was disposed, and non-attached cells were removed. (Podinovskaia and Descoteaux 2015). Then 200 µL DMEM medium were added in all the 96 wells of the plate. In row H extra medium for the vertical serial dilution step was added. Aliquots of compound stocks were added at different initial concentrations depending on the substances, in row H and then 1:3 or 1:5 vertical serial dilution was conducted, starting from row H to row C disposing the final transfer volume. Triplicates were measured for each compound. The plate was incubated for another 24 h at 37 °C and 5 % CO₂. Afterwards 50 µL of resazurin solution (final concentration in wells 20 µM) was added and after 4 h of incubation, the fluorescence was measured at 560 nm excitation and 590 nm emission using a plate reader (Perkin Elmer Enspire, Germany). From plots of the viability and the compound concentration IC₅₀ values were determined using a four-parameter logistic model by a custom designed Excel worksheet with Python support.

2.5 UV detection of cycloreversion in AcEPs

A sample of the corresponding Ac in 1.5 mL ethanol (final concentration ranging from 2, 8 and 10 µM) was transferred into a quartz cuvette and measured by an Uv/vis-spectrometer (Hitachi U3300) at 70 °C. After this measurement, an aliquot of the corresponding AcEP substance within ethanol (final concentration 40 µM) was pipetted in a cuvette and its Uv spectra were measured at 70 °C in a time interval of 1 h during a period of 24 h. After measurements, the re-appearance of the Ac absorption pattern was verified.

2.6 Formation of the xylenol/Fe³⁺ complex by EP

The color reagent was prepared with xylenol orange (XO) (125 µM) and butylated hydroxytoluene (4 mM) dissolved in methanol/H₂O (9:1) and immediately before use FeSO₄ (25 mM) in 2.5 M H₂SO₄ was added, giving it a final concentration of 250 µM FeSO₄ in the samples. In a 1.5 ml cuvette (BRAND, Wertheim, Germany) an aliquot of the EP solution (100 µM final concentration) was mixed with 1 mL of the color reagent. The slower reacting EPs were incubated at 25 °C and spectra in the range of 400 nm – 650 nm were recorded in 1 min intervals for 30 min using a MS1501 UV-VIS diode array spectrophotometer (Shimadzu, Japan). A solution of methanol: H₂O (9:1) was used as a reference. The faster reacting EPs were scanned every 5 s during a period of 5 min. The OD difference of the sample at 560 nm and 650 nm was determined at each time interval. The slope of the reaction was converted to concentration change (formation of Fe³⁺) by an extinction coefficient of the XO/Fe³⁺ complex: 15000 l * mol⁻¹ * cm⁻¹.

2.7 Detection of superoxide radicals by CMH/EPR

An aliquot of the LtP cell culture containing 5×10^8 LtP was transferred into a 15 mL Eppendorf tube and was centrifuged (Hettich Universal 16) at 20 °C with 2000×g speed. The supernatant was discarded, the cell pellet was resuspended in 3 ml PBS with 15 mM glucose and centrifuged. The cells were resuspended again in 3 ml PBS with 15 mM glucose after the removal of the supernatant. Four aliquots of 500 µL of this cell suspension were transferred into 1.5 mL Eppendorf tubes. Samples containing PBS/glucose or only LtP were used as negative controls. AcEP (100 µM final concentration) and the corresponding non-endoperoxide Ac (100 µM final concentration) were pipetted in two of the four 1.5 mL Eppendorf tubes containing 500 µL LtP cell suspension. All the aliquots were incubated for 20 min at 27°C. Then AA (0.8 µM final concentration) was added to the respective aliquot, before measurement. Prior to measurement the mixture of DFO (100 µM final concentration) and DTPA (25 µM final concentration) and CMH (400 µM final concentration) was added in each tube. An aliquot was aspirated into a capillary (50 µL) located in the MD5 resonator of the EPR spectrometer (Bruker, EMX Digital Upgrade). The measurement was started using following parameters: microwave frequency 9.682 GHz; microwave power 20 mW, modulation frequency 100 kHz; modulation amplitude 1 G; center field 3448 G; sweep width 100 G; attenuation 70dB. Four replicates for each sample were measured as fast as possible in time intervals of 0, 20, 45 and 60 min to calculate CMH oxidation rate. Besides the two Ac/AcEPs sample types, always a group with LtP (100 %), buffer only and LtP + AA was included to guaranty the proper function of the assay. Finally, CHM oxidation rates over this time period were expressed in relation to the LtP sample (100 %). The values of two measurement sessions were averaged.

2.8. Data analysis

Calculations and graphing were carried out using Excel (Microsoft). Mean and standard derivation (SD) were calculated for each experiment. The number of replicates is shown at the corresponding figures/tables. IC_{50} values were calculated from non-linear concentration-response curves using a four-parameter logistic model and expressed as the mean \pm SD (Müllebnner et al. 2010).

3. Results

3.1 Method development

3.1.1. Single compound assays

The first objective of the work was to establish new methods for viability assays of prospective antileishmanial compounds. The horizontal viability assay (Figure 8) developed in this work, has the advantage of having a wider range of concentrations (12 different concentrations for each compound) compared to the vertical viability assay which has only 6 different concentration per compound. The wider range of concentration increases the accuracy of the IC_{50} values calculated for this viability assay. This is essential to perform combination viability assays.

3.1.2. Combination viability assay

The second method developed, was the combination viability assay (Figure 9) to study the interaction of two drugs in LtP, as a synergistic drug combination could have a greater efficacy compared to the outcomes of individual drugs. Combinations of compounds that shows synergy allow dose-increase to boost the efficacy and dose-decline to lessen the side effect. In addition, synergy could prevent the development of resistant strain. However, the challenge of this method is the massive number of possible combinations and the complicated plate setup (Cokol-Cakmak 2018). Only for the compounds tested in this work (15 compounds) there would be 32768 (2^{15}) potential groupings. This would take years to accomplish.

IC_{50} values (Figure 10) of each single compound were assessed. Then the IC_{50} values of each compound in combination were determined (Figure 11). According to Equation 1, FIC values were calculated. If the values were below 0.5, compounds showed synergism, values above 1 indicated an antagonism.

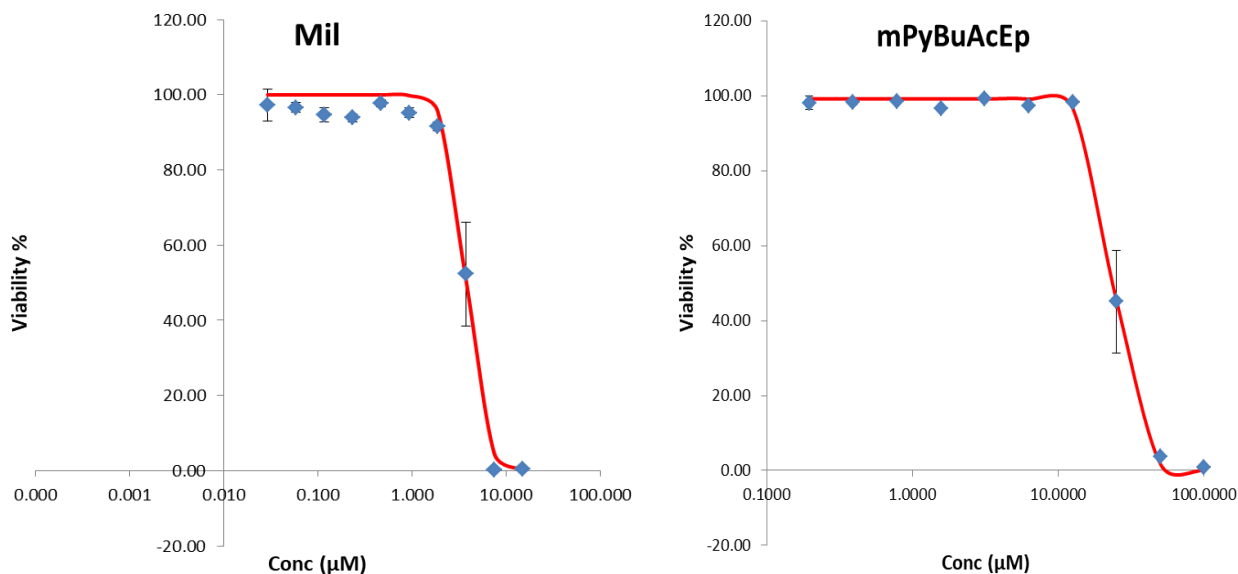


Figure 10. Concentration-viability curve of combination viability of as a function of different concentrations of Mil (left) (15 μM - 0.029 μM) and mPyBuAcEP (right) (100 μM - 0.195 μM). The IC_{50} value obtained from this experiment for Mil was $3.77 \pm 0.14 \mu\text{M}$ and for mPyBuAcEP was $24.24 \pm 0.79 \mu\text{M}$. Individual data points represent mean \pm SD of duplicate measurements.

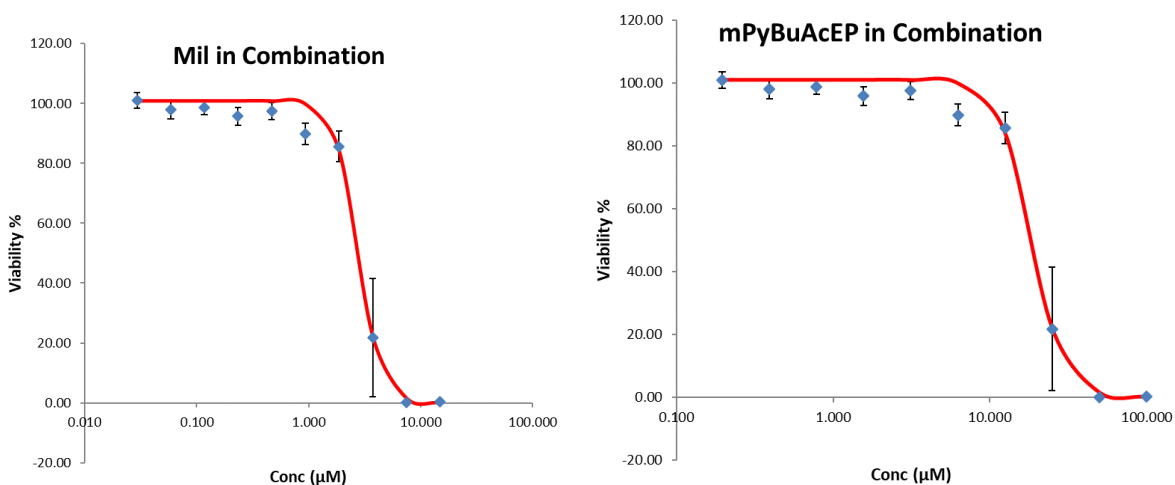


Figure 11. Concentration-viability curve of Mil in combination and mPyBuAcEP in combination represent the effect on IC_{50} values of each compound in combination. Left graph shows the effect that the presence of mPyBuAcEP changed the IC_{50} value of Mil to $2.76 \pm 0.13 \mu\text{M}$. Right graph shows that Mil changed the IC_{50} value of mPyBuAcEP to $18.43 \pm 0.88 \mu\text{M}$.

In this example the possible synergy of Miltefosine (Mil) with mPyBuAcEP was studied. The IC_{50} value of Mil alone at 3.77 μM shifted to 2.76 μM in the presence of mPyBuAcEP (Figure 10, 11). The IC_{50} value of mPyBuAcEP alone at 24.24 μM shifted to 18.43 μM in the presence of Mil (Figure 10, 11). FIC value for this the example was 1.49. The displayed experiment with Mil and mPyBuAcEP showed no synergy between the substances tested.

3.2 Influence of EPs and non-EPs on viability of LtP and J774

During the study, IC_{50} values of the EPs and non-EPs for both LtP cells and J774 macrophages were determined from the viability assays. In Figures 12 and 13 examples of concentration viability curves for an AcEP and a non-peroxidic analog are shown. Pentamidine was used as a positive control compound. Most EPs appeared to be relatively toxic to the LtP cells. But some of these substances also showed toxicity to J774 macrophages. In Table 4. are listed all the compounds tested, their respective IC_{50} values and selectivity towards LtP or J774 cells.

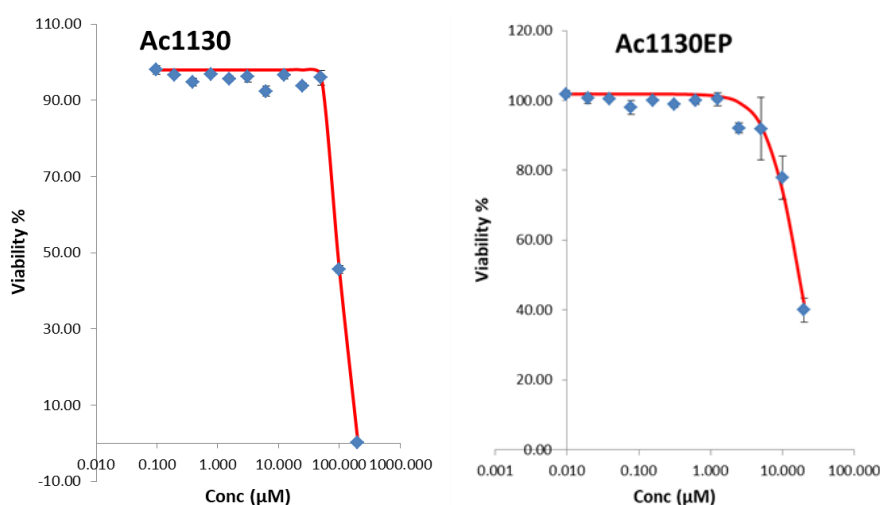


Figure 12. Concentration-viability curve of the horizontal viability assay of LtP as a function of different concentrations of Ac1130 (left) (from 200 μM to 0.098 μM) and its EP (right) (from 20 μM to 0.01 μM). The IC_{50} values obtained from this experiment for Ac1130 was $97.8 \pm 1.8 \mu\text{M}$, while for Ac1130EP was $16.6 \pm 1.0 \mu\text{M}$. Individual data points represent mean \pm SD of duplicate measurements.

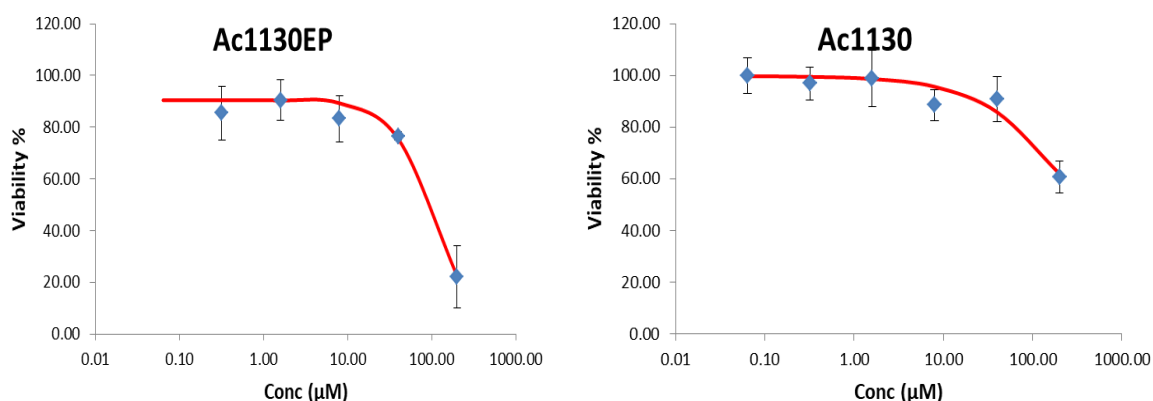


Figure 13. Concentration-viability curve of the horizontal viability assay of J774 macrophages as a function of different concentrations of Ac1130EP (left) (0.06 μM , 0.32 μM , 1.60 μM , 8.00 μM , 40 μM , 200 μM) and its corresponding non-EP (right), (Ac1130EP 0.06 μM , 0.32 μM , 1.60 μM , 8.00 μM , 40 μM , 200 μM). The IC_{50} values obtained from this experiment for Ac1130EP was $104.0 \pm 0.4 \mu\text{M}$, while for Ac1130 it was $>200 \mu\text{M}$. Individual data points represent mean \pm SD of triplicate measurements.

Table 4. IC₅₀ values and selectivity of EPs and their corresponding non-EPs in LtP and J774 cells. The IC₅₀ values were determined by using resazurin viability assay in 96 well plates. Pen is an established antileishmanial compound and was used as a reference compound in these experiments. Data represent mean \pm SD of 3-9 individual experiments.

Endoperoxide Compounds	LtP	J774	Selectivity
	IC ₅₀ (μ M) Mean \pm SD	IC ₅₀ (μ M) Mean \pm SD	IC ₅₀ of J774 / IC ₅₀ of LtP
Pen	1.99 \pm 2.52	17.1 \pm 2.7	8.5
Ac	>200	>200	-
AcEP	19.7 \pm 14.1	1.217 \pm 0.325	0.06
Ac1118EP	21.1 \pm 1.7	2.86 \pm 1.25	0.13
Ac1130	83.0 \pm 17.2	>200	>2.4
Ac1130EP	9.05 \pm 8.24	84.1 \pm 56.2	9.2
DPAc	197 \pm 92	136 \pm 35	0.7
DPAcEP	9.67 \pm 2.15	195 \pm 117	20.1
mPyBuAc	0.294 \pm 0.126	32.6 \pm 6.8	110
mPyBuAcEP	1.27 \pm 1.19	23.3 \pm 8.8	18.2
oPyAc	>200	>200	-
oPyAcEP	5.32 \pm 2.60	3.22 \pm 3.01	0.6
oPy2C8AcEP	14.4 \pm 7.0	13.9 \pm 3.4	0.9
pPyBuAc	1.86 \pm 1.10	107 \pm 46	58
pPyBuAcEP	0.707 \pm 0.662	26.1 \pm 10.6	37

3.3 Measurement of superoxide radicals by CMH/EPR

To elucidate the mechanism of action of AcEPs in LtP, measurements of superoxide radical formation in LtP were conducted. AcEPs form radicals in LtP, which can lead to oxidative stress and formation of superoxide radicals in LtP. CMH reacts with superoxide radicals under formation of the stable CM[•] radical (Figure 14), which can be detected by EPR spectroscopy (Figure 15). CMH oxidation rates over time periods of 0, 20, 45 and 60 min were measured in relation to the LtP sample. The experiments were performed in the presence of AcEPs, their corresponding non-EPs in PBS/glucose buffer containing LtP and the iron chelators DFO and DTPA (not during incubation with AcEPs). LtP only samples were used as internal reference (100 %). LtP with AA (a trigger of mitochondrial superoxide formation) served as positive control (Figure 16)

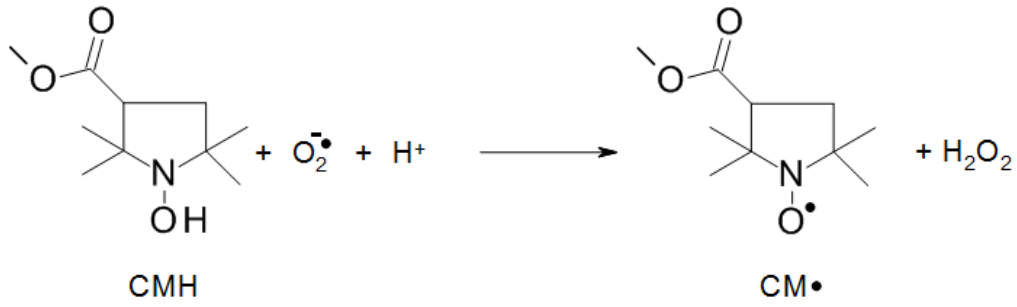


Figure 14. Reaction of CMH with superoxide radicals O₂^{•-} forming the stable radical CM•, detected by EPR spectroscopy.

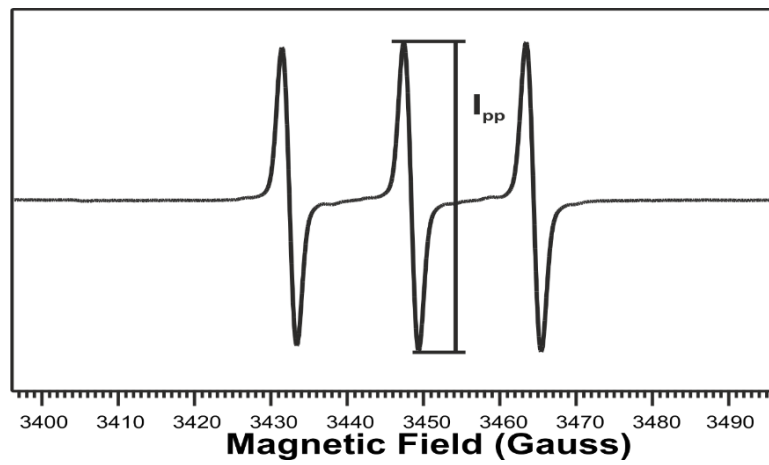
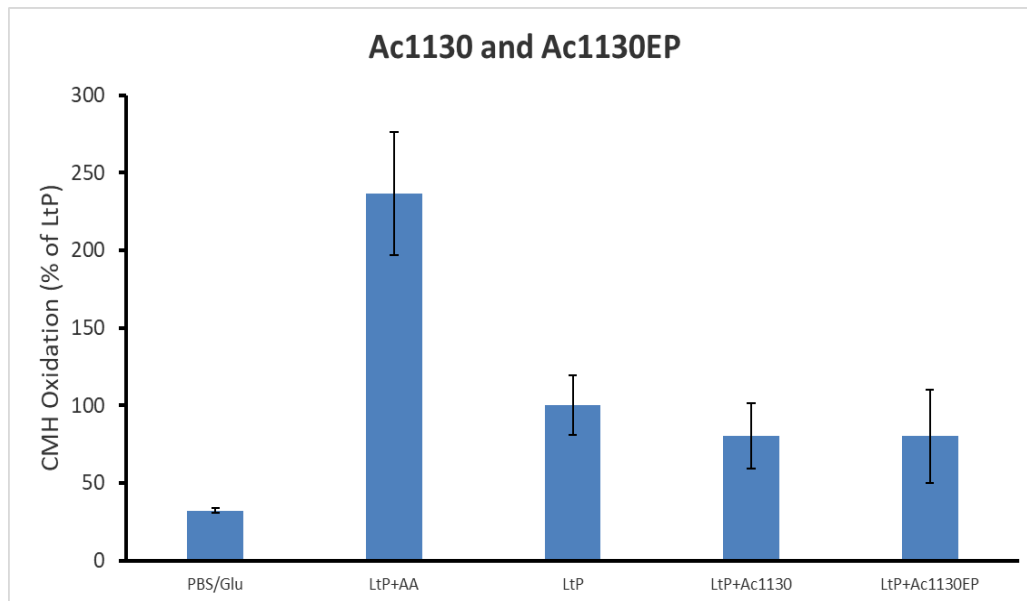
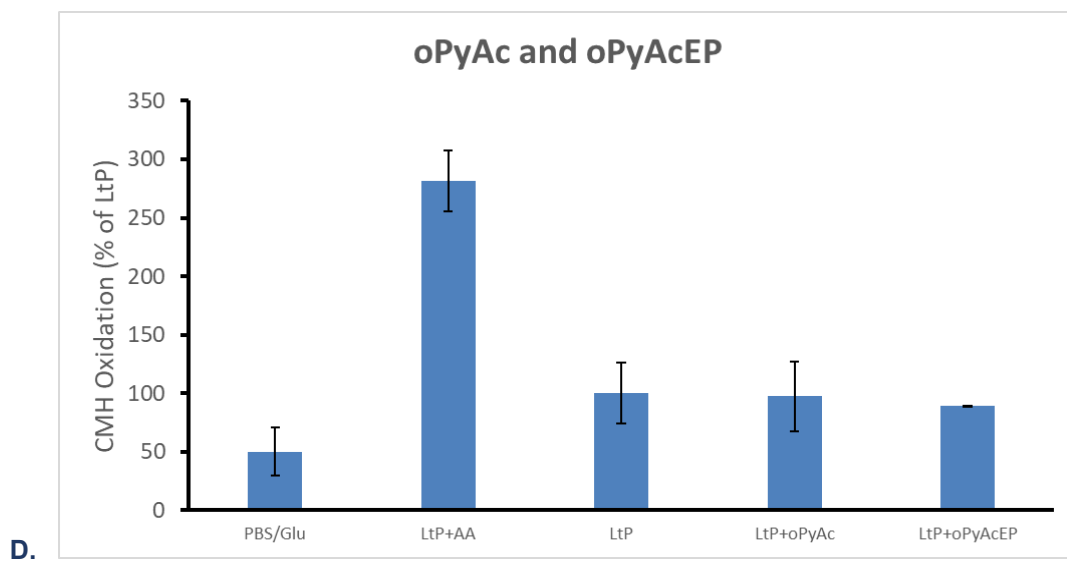
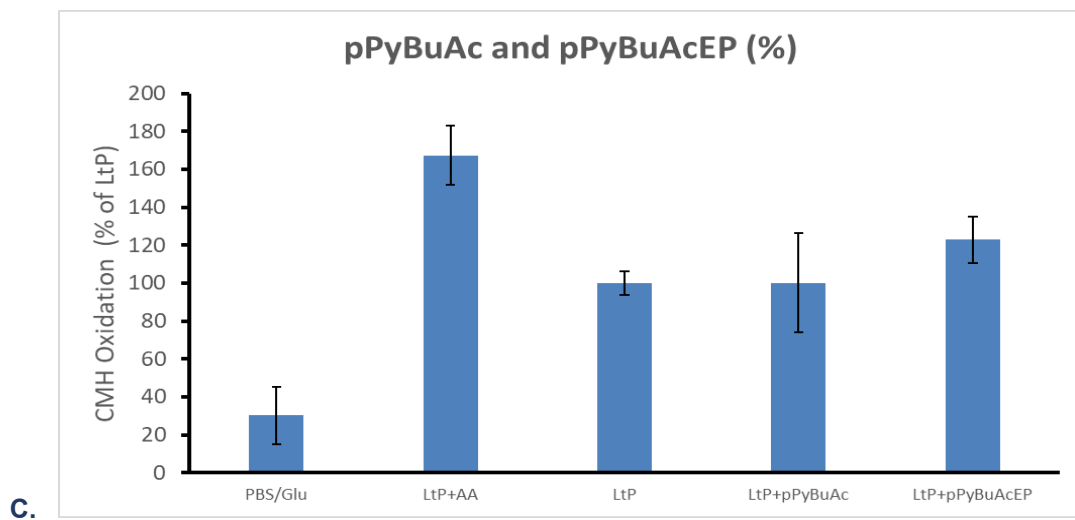
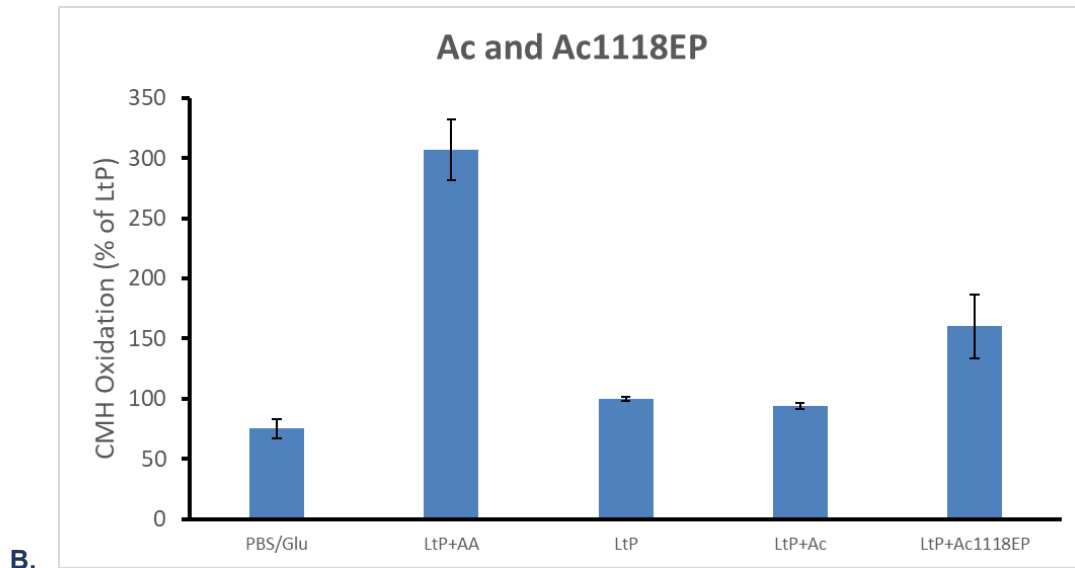


Figure 15. EPR spectrum of CM• obtained from CMH oxidation. The peak-to-peak intensity (I_{pp}) which was used for quantification is indicated.





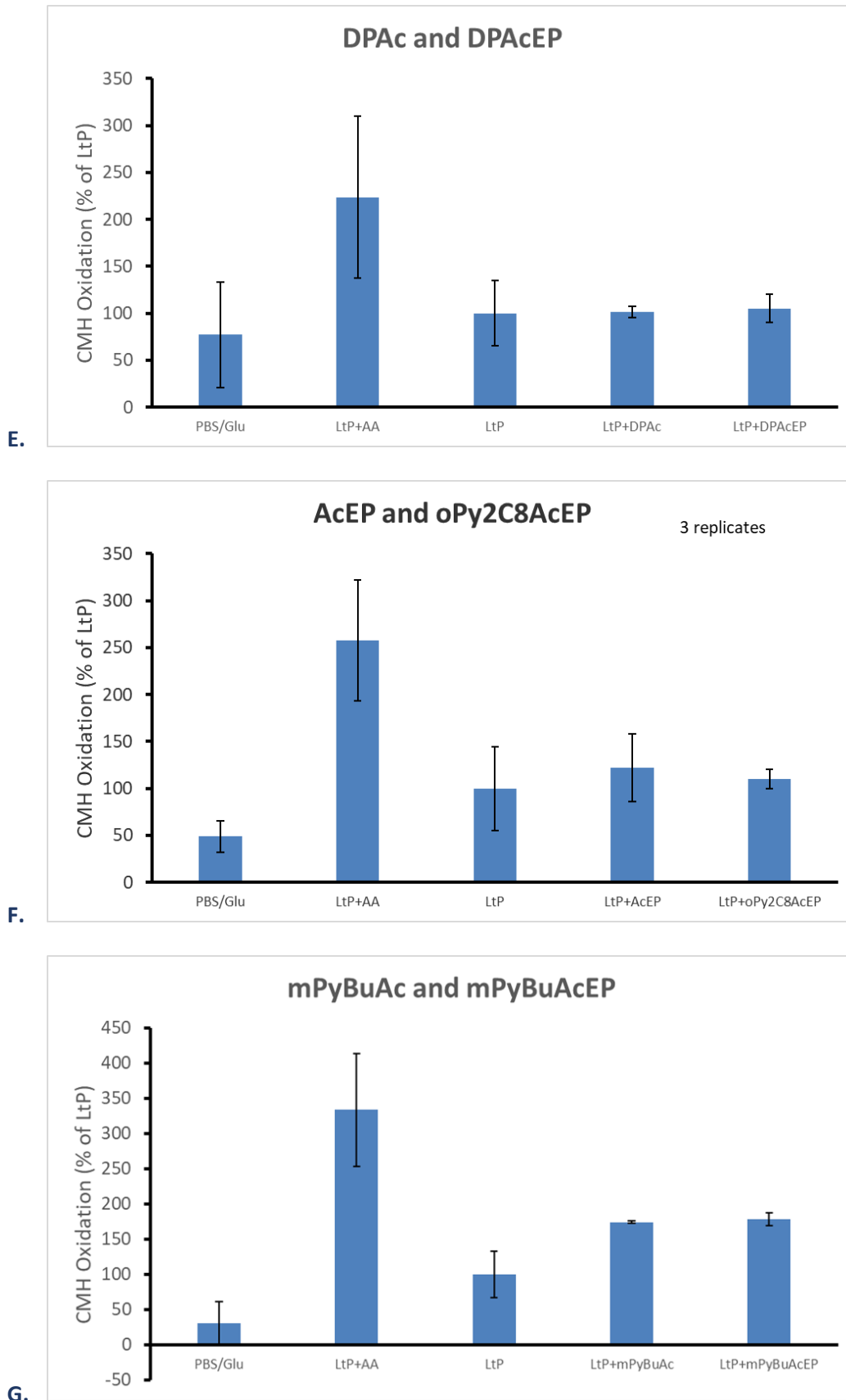


Figure 16. CMH oxidation (% of LtP) in the presence of AA or Ac (A: Ac1130 B: Ac1118; C: pPyBuAc; D: oPyAc; E: DPAC; F: AcEP; G: mPyBuAcEP) or AcEP (A: Ac1130EP; B: Ac1118EP; C: pPyBuAcEP; D: oPyAcEP; E: DPACeP; F: oPy2C8AcEP; G: mPyBuAcEP) (each 100 μ M). PBS/Glucose represents a control experiment without LtP. LtP represents a control experiment without additional compounds. Data represent mean \pm SD of 2-3 independent experiments.

Most AcEPs and analogs did not trigger additional superoxide radical formation in LtP within 20 min of incubation. Exceptions are Ac1118EP and pPyBuAcEP which caused additional superoxide radical production in LtP.

3.4 Chemical reaction mechanisms of AcEPs

3.4.1 Reactivity of EP with FeSO₄

The reactivity of EPs regarding Fe²⁺ was quantified by the formation of Fe³⁺ through complexation with the color reagent XO (Figure 17,18). The rates of the reaction of EPs and their analog non-EPs with FeSO₄ are shown in Figure 19. The non-EP did not react with Fe²⁺. Compared to the non-EP, most EPs reacted with the Fe²⁺, some at higher rates than the others.

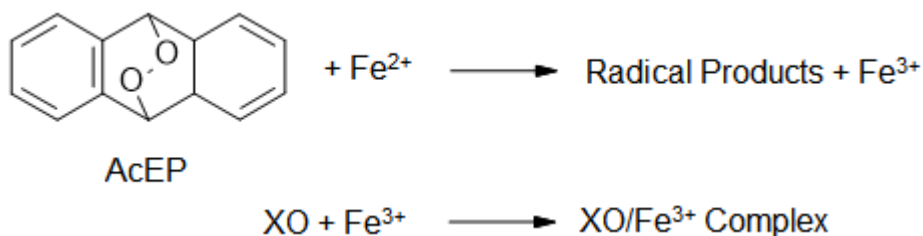


Figure 17. The reaction of AcEP decomposition by Fe²⁺. Fe²⁺ triggers AcEP cleavage into radical products and Fe³⁺. Fe³⁺ forms a complex with XO, which allows to measure the rate of Fe³⁺ formation.

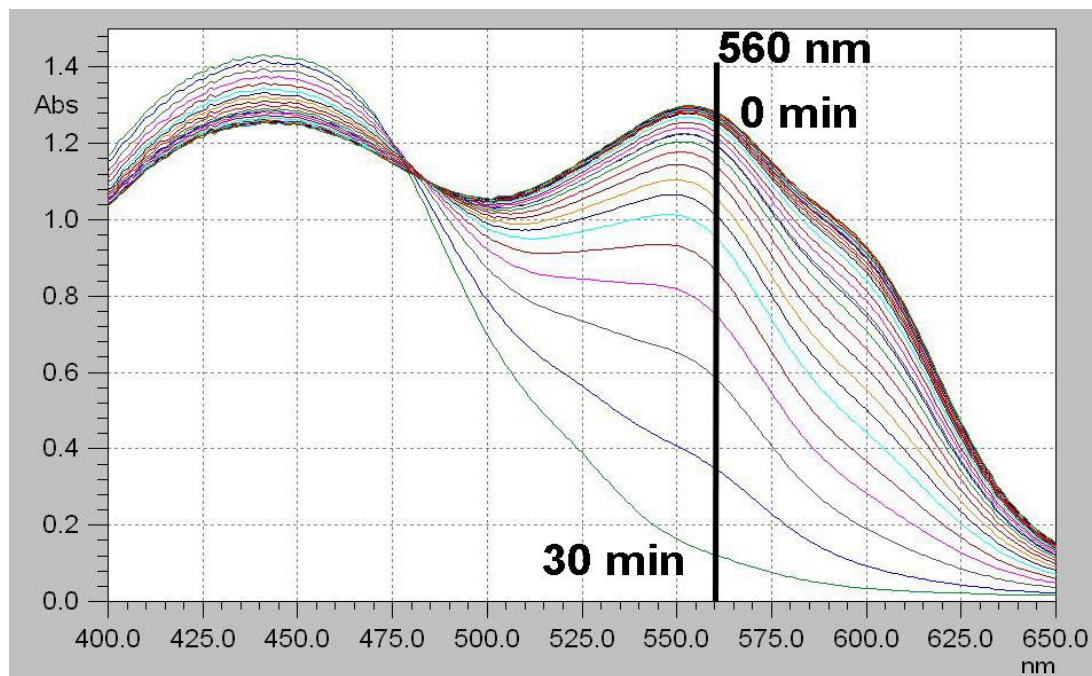


Figure 18. The spectra of the XO/Fe³⁺ complex formation in the presence of 100 μM oPyAcEP.

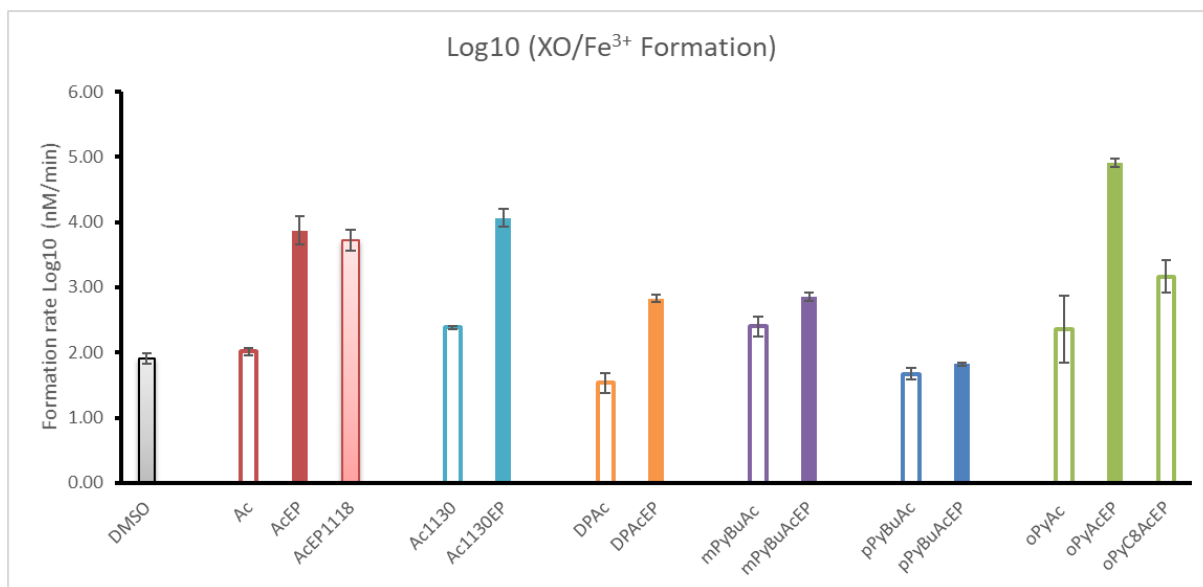


Figure 19. Formation rate of the xylenol/ Fe^{3+} complex by EPs (final concentration $100 \mu\text{M}$). Data represent mean \pm SD of three experiments.

3.4.2 UV detection of cycloreversion

In the last experiments of this study the potential of EPs to undergo cycloreversion was determined (Figure 20). Figures 21-25 show spectra of the individual AcEP during their thermal decomposition along with their non-peroxidic parent compound. Table 5. shows which compound underwent cycloreversion to its non-EPs analog.

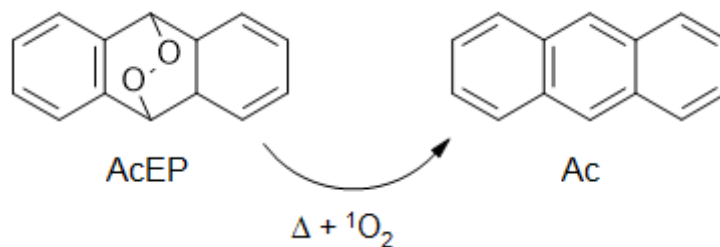


Figure 20. The concept of AcEP undergoing cycloreversion and releasing singlet oxygen by heating.

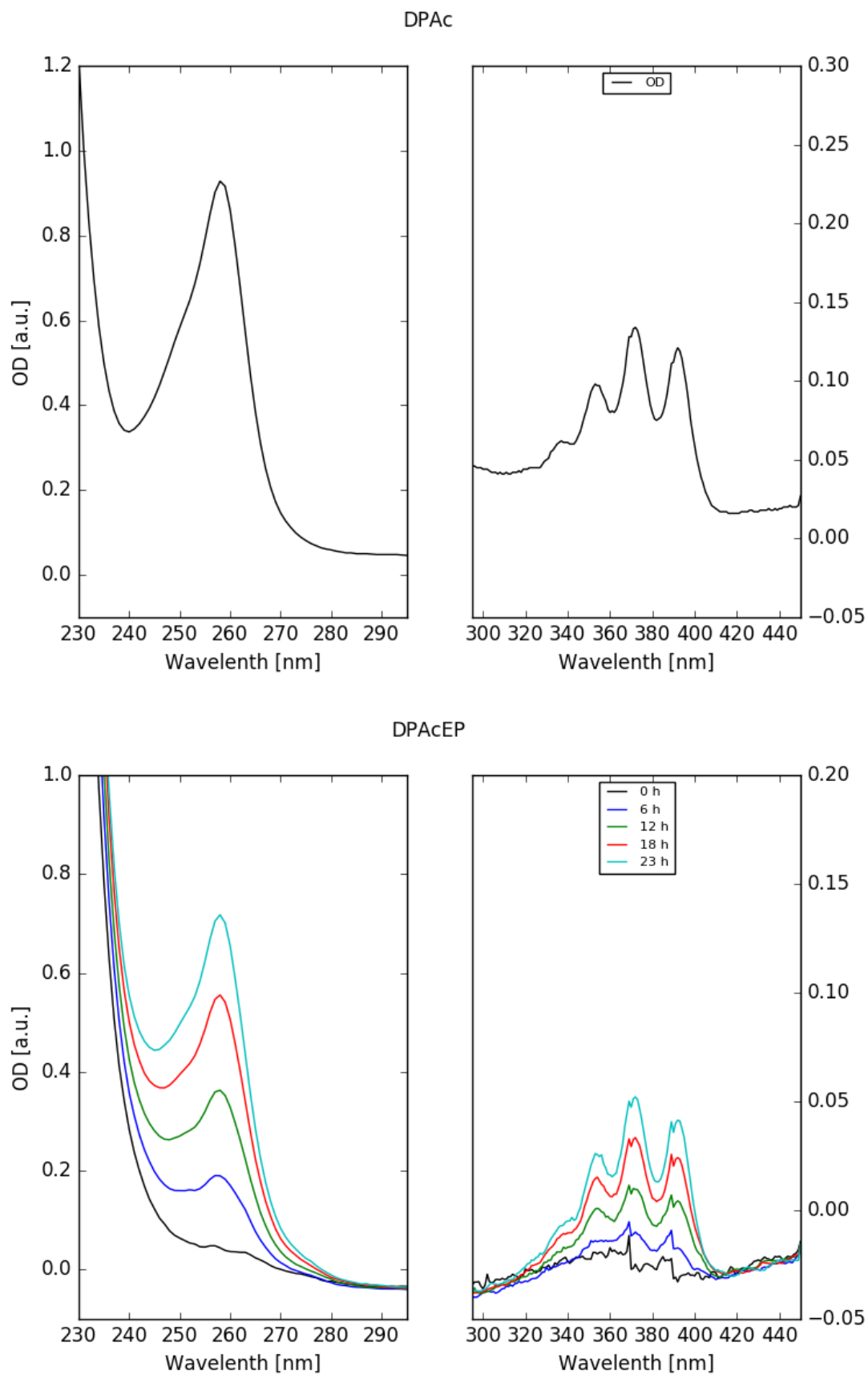


Figure 21. UV spectra of DPAc (top) ($8 \mu\text{M}$) and DPACeP (bottom) ($40 \mu\text{M}$) after heating for 0, 6, 12, 18 and 22 h.

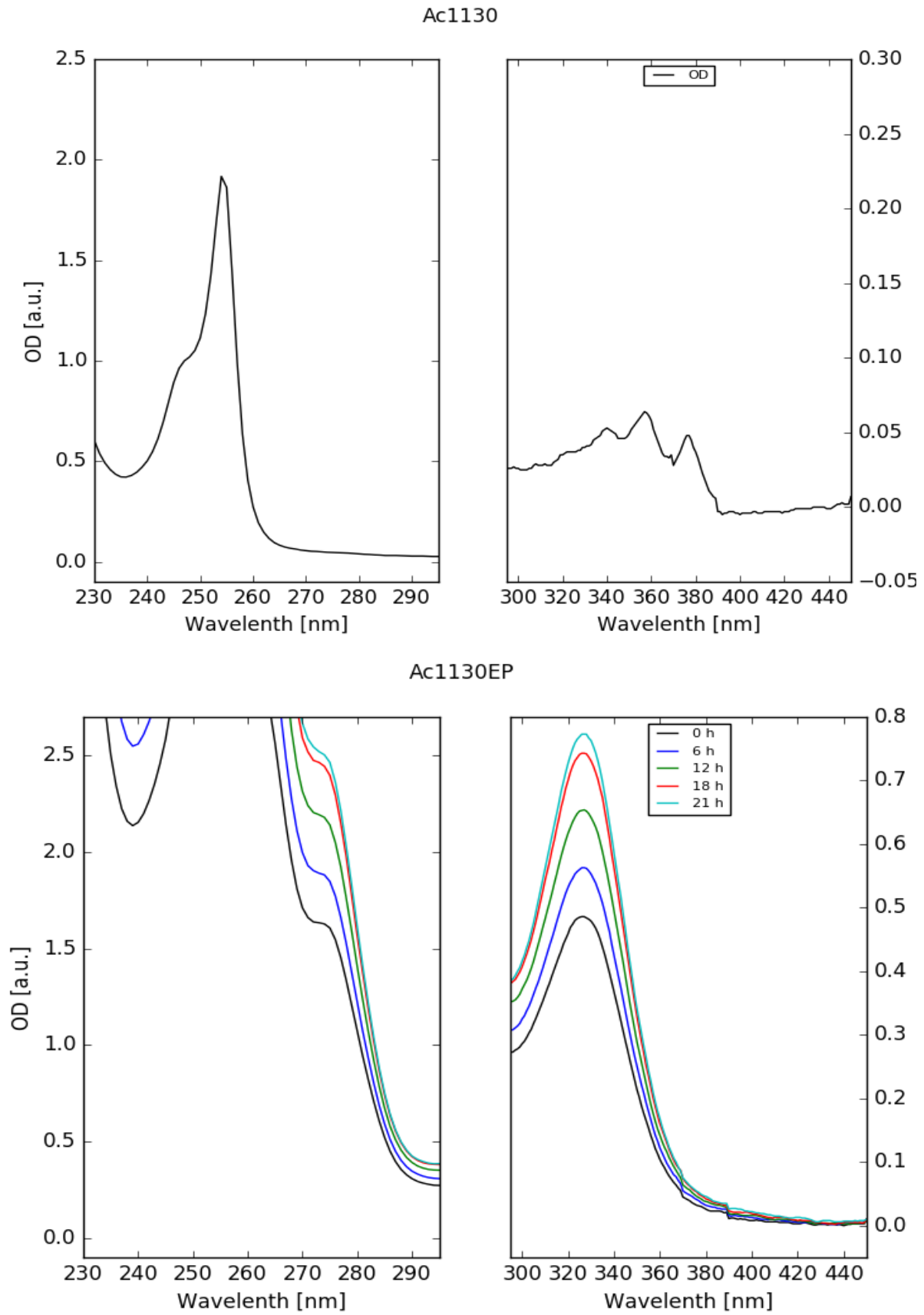


Figure 22. UV spectra of Ac1130 (top) (8 μM) and Ac1130EP (bottom) (40 μM) after heating for 0, 6, 12, 18 and 21 h.

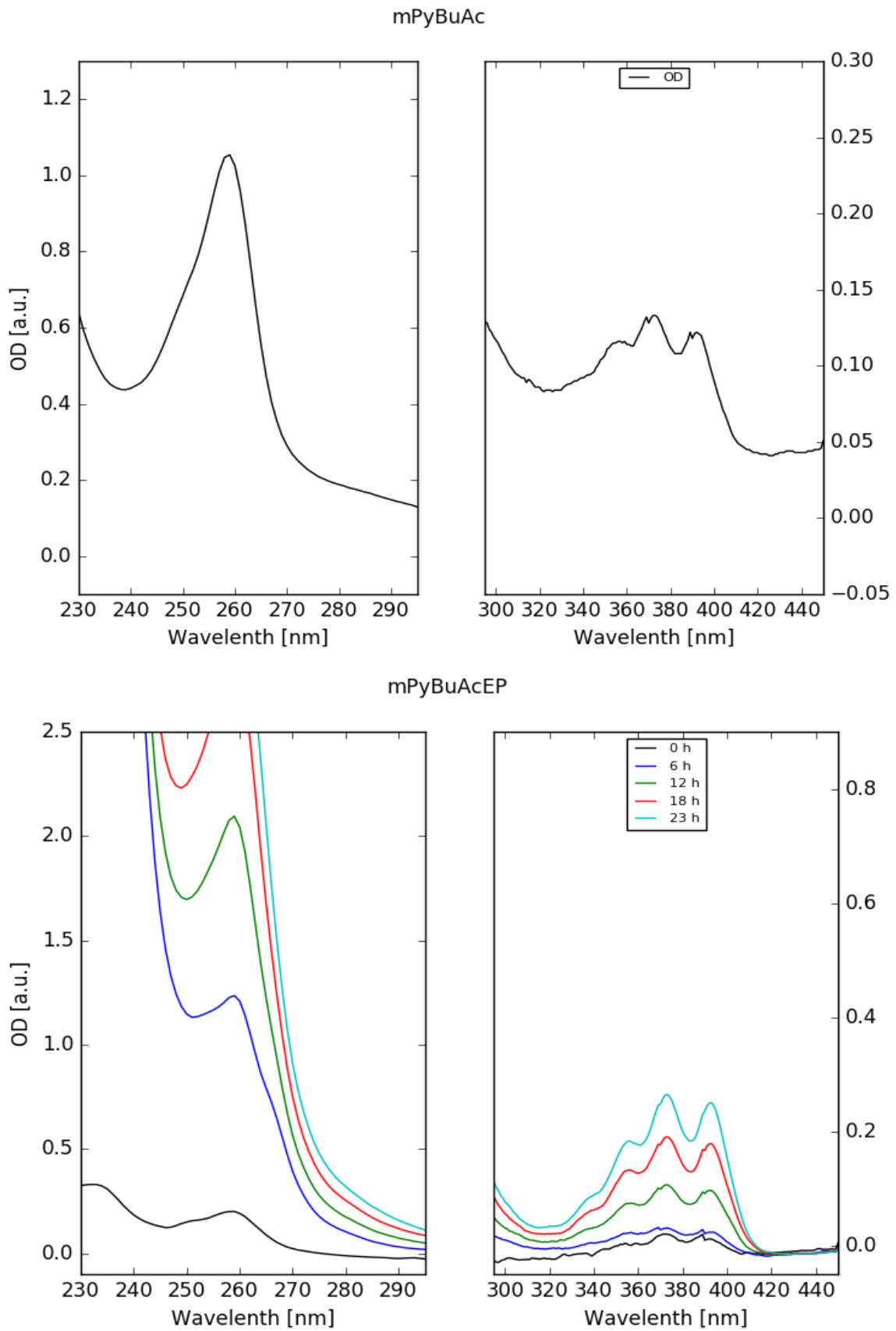


Figure 23. UV spectra of mPyBuAc (top) (2 μM) and mPyBuAcEP (bottom) (40 μM) after heating for 0, 6, 12, 18 and 23 h.

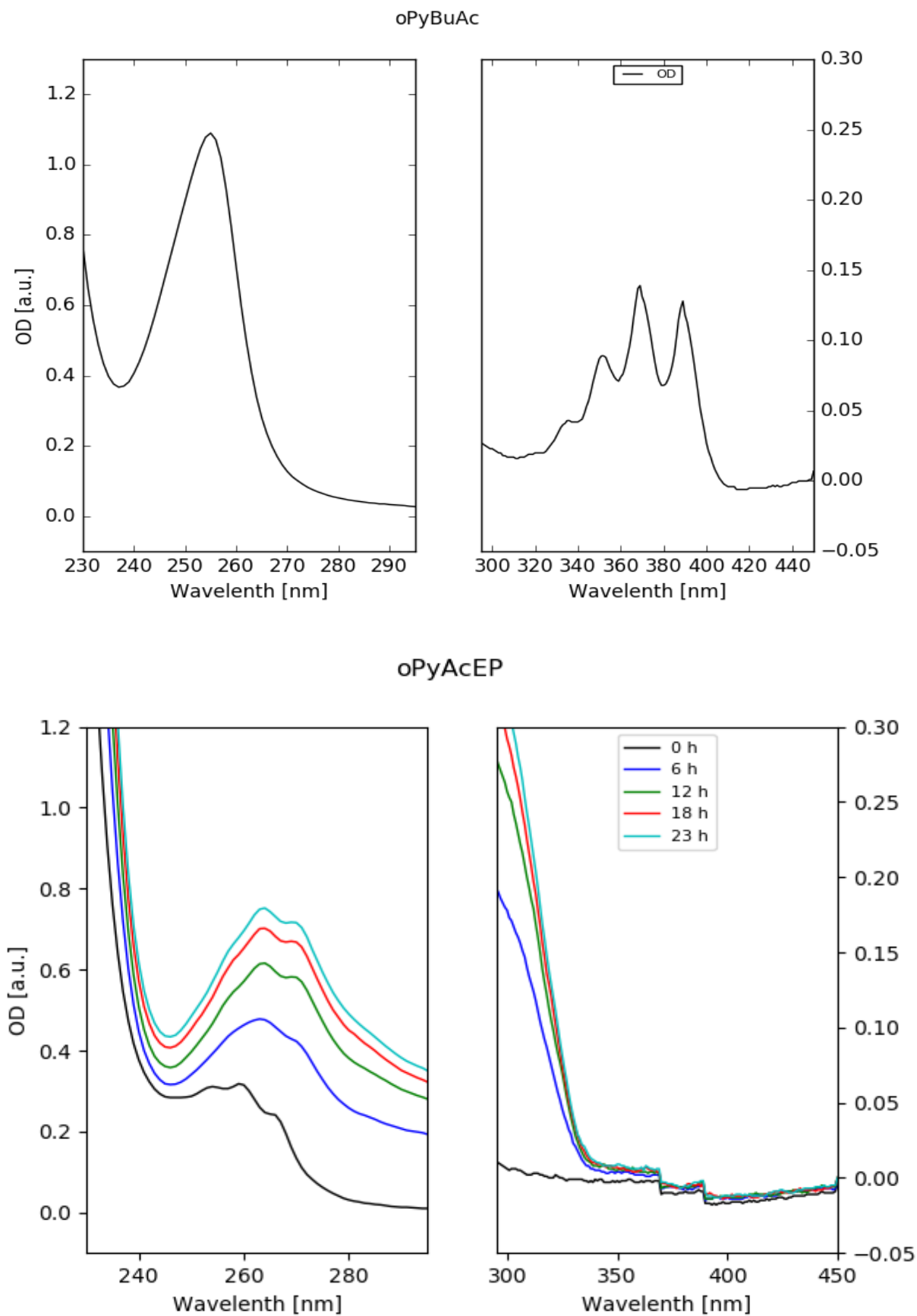


Figure 24. UV spectra of oPyAc (top) ($8 \mu\text{M}$) and oPyAcEP (bottom) ($40 \mu\text{M}$) after heating for 0, 6, 12, 18 and 23 h.

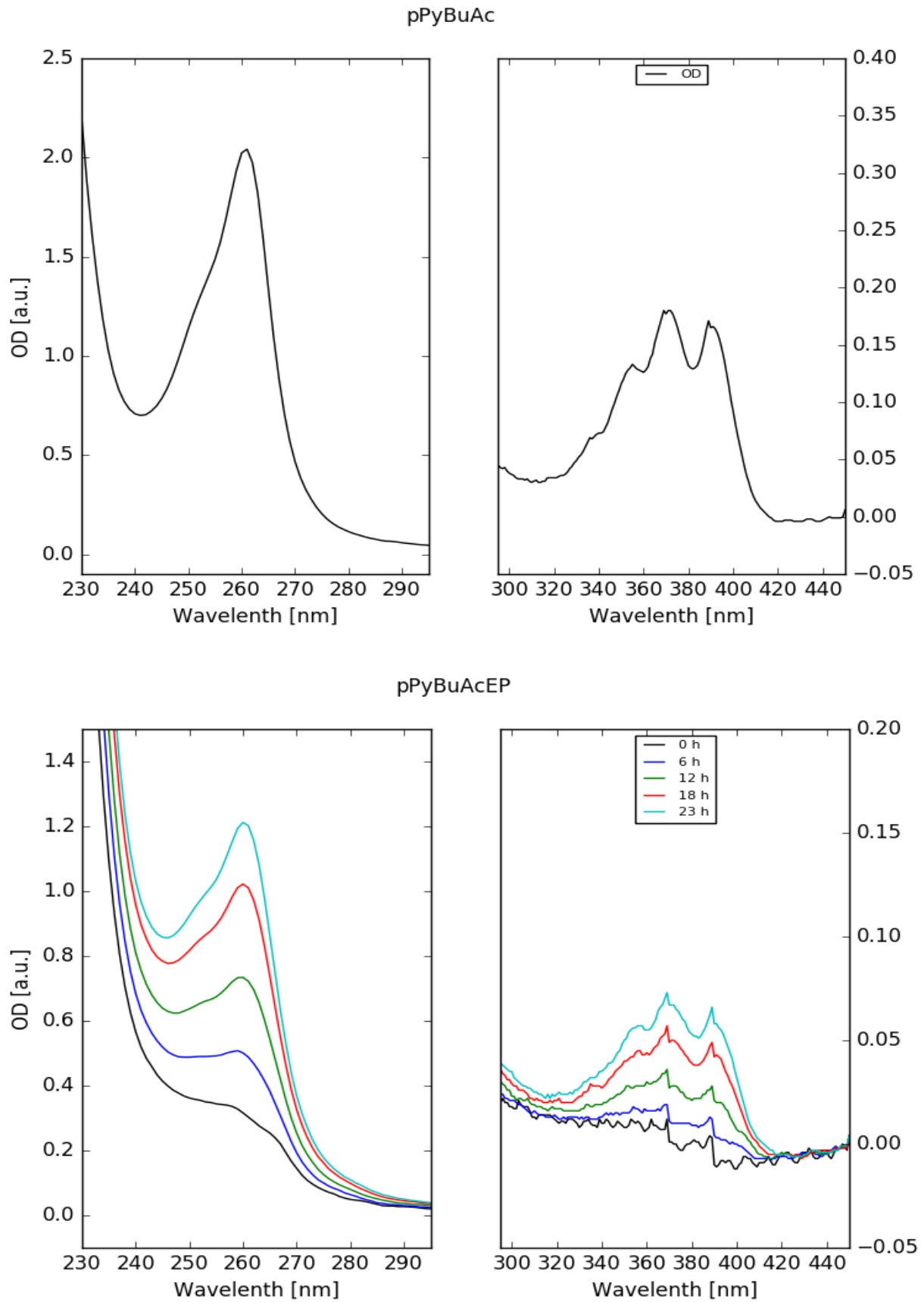


Figure 25. UV spectra of pPyBuAc (top) (8 μM) and pPyBuAcEP (bottom) (40 μM) after heating for 0, 6, 12, 18 and 23 h.

Table 5. EPs studied and their ability to undergo cycloreversion based on the UV spectra of the EPs and their corresponding non-EPs.

Endoperoxide Compounds	Cycloreversion
Ac1130EP	no
DPAcEP	yes
mPyAcEP	yes
oPyAcEP	no
pPyBuAcEP	yes

Some of the molecular more complex AcEPs undergo cycloreversion, while a molecular simpler AcEP, such as Ac1130EP, has other thermal decomposition pathways.

4. Discussion

Leishmaniasis is a global disease, mainly occurring in tropical and subtropical regions. Because of the vector-borne characteristics of this disease, the distribution is dependent on the endemic area of sandflies as vectors and the reservoirs in mammalian hosts. Due to climate change the endemic area of sandflies is expanding to previously non-endemic regions, which means in Europe from the Mediterranean area further north and is also becoming a threat for countries like Austria.

The problems of this disease complex are the variety of *Leishmania* species and its different clinical manifestations. Because of socioeconomic problems in endemic regions, such as India and Brazil, the availability of drugs, which are cheap, have no toxic side effects and are easy to apply is limited. Therefore, *Leishmania* research to find new effective drugs is ongoing. In previous publications (Menezes et al. 2015), it was shown that the Essential oil of *Chenopodium ambrosioides* has substantial antileishmanial properties in vitro and in a mouse model of cutaneous leishmaniasis in vivo. A major ingredient of this oil is the endoperoxide ascaridole, which has also in vitro and in vivo anti-leishmanial properties. This triggered the search for other natural and synthetic endoperoxides with antileishmanial activity.

This thesis focused both on the improvement of research methods and the exploration of the activity of a set of AcEPs and their possible mechanisms.

The backbone of in vitro identification of antileishmanial compounds are cellular model systems, which represent *Leishmania* on the one side, such as LtP, and macrophages on the other side, such as J774 macrophages. The basic element to test new compounds in cell lines are viability assays. These assays provide concentration-viability curves, from which IC₅₀ values can be deduced. In a non-robotic laboratory, the format of 96 well plates is typical to perform these tests. However, to guarantee a sufficient throughput (ten plates or more per day) for screening purposes, the plate layout chosen for the experiment is of central importance. Usually, these plates have to exhibit control wells with medium only (0 % viability) and with cells only (100 % viability). In addition, to create concentration-viability curves, a number of compounds in different concentrations is placed in the plates. To enable effective manual loading without robots the principle of serial dilution is applied. The classical plate layout (Figure 7), which was used in our laboratory over the last years consisted of two control rows and four blocks of different compounds in decreasing concentrations from row H to row C, which were prepared by serial dilution. The advantage of this layout is that concentration- viability curves of four different compounds per plate in triplicate experiments can be obtained providing a high throughput. This enables basic determination of IC₅₀ values in the respective cell types. However, this plate layout has also some important limitations.

Although with completely new compounds usually a 1:5 serial dilution with 200 μM as initial concentration provides a good overview about the compound activity, the obtained IC_{50} values have a high standard deviation between different preparations of the same compound at the same concentration. Therefore, after this initial plate with 1:5 dilution, often the initial concentration was changed and only a 1:3 dilution was applied to obtain a denser concentration grid. The requirement for this adjustment comes from the recommendation that for IC_{50} determination, a sufficient number of data points both above and below 50 % viability are required (Sebaugh 2011). Lower dilution values than a 1:3 ratio are not possible with this procedure since this ratio already requires a 100 μL transfer volume with a final assay volume of 200 μL , which sums up to 300 μL during serial dilution and is close to the volume limit of the wells of 340 μL . Therefore, to achieve a higher precision of the IC_{50} values both changes of the plate layout and lower dilution ratios are required.

Therefore, a plate layout with horizontal serial dilution (Figure 8) was established containing control wells in rows A and H. Three compounds in duplicates were distributed from row B row G with the highest concentration in column 1 and a serial dilution with 12 steps. To achieve a 1:2 concentration ratio the serial dilution was performed with a lower volume (100 μL) of medium and subsequent addition of cells after serial dilution, giving the required 200 μL total volume. This setup provided more accurate concentration-viability curves and sufficient data points above and below 50 % viability resulting in more accurate IC_{50} values.

Besides the study of single compound actions on *Leishmania* and host cells, possible synergies of antileishmanial compounds are of interest. This is based on the fact that a part of this research arose from the study of essential oils, which are compound mixtures per se. For example, it has been shown that the efficiency of ascaridole and of the essential oil of *Chenopodium ambrosioides* against leishmania is in the same range, however the essential oil possessed a lower toxicity in macrophages than ascaridole alone (Monzote et al. 2014). Likewise, from antibacterial drug research it is known that identification of synergies can be important. To address this problem in vitro, we developed and established a viability combination plate assay (Figure 9). This plate layout is based on a horizontal serial 1:2 dilution and contains control wells in column 1 and 12. In a combination plate the possible synergy of two compounds can be studied. The compounds were applied separately in duplicates in rows A to D and in combination in quadruplicates in rows E-H with the highest concentration in column 2. This setup gave 10 different concentration-viability data pairs in a 1:2 concentration grid, which was required to identify also smaller synergistic effects. Within this thesis only some pilot experiments have been performed to ensure the practicability and accuracy of the setup. Based on this plate layout IC_{50} values for the separate compounds were obtained (Figure 9 and 10). Furthermore, the IC_{50} values of the compounds alone and in combination with the other compound were analyzed by calculating the respective IC_{50}

values from the combination wells (Figure 11). This was used to calculate the fractional inhibitory index (FIC) (Equation 1). An FIC below 0.5 is considered as synergistic combination. More studies with this methodology will be performed in future.

In the second part of this work a compound set of newly synthesized AcEPs and their corresponding non-peroxidic analogs (Ac) were studied (Figure 6). The obtained IC_{50} values in LtP and J774 macrophages demonstrated a broad range of activity (Table 4). The quality control pentamidine showed a low micromolar IC_{50} value in LtP and an IC_{50} around 20 μ M in J774 macrophages giving a selectivity close to 10. For a part of the AcEPs it is clearly visible that the compound with the endoperoxide (AcEPs) has a higher activity against leishmania than the non-peroxidic analogs (Ac). This group includes compound pairs, such as Ac/AcEP, Ac1130/Ac1130EP, DPAC/DPACEP and oPyAc/oPyAcEP. However, an unwanted property of these compounds pairs is their toxicity in J774 cells resulting in a low selectivity. Especially AcEP, oPy2C8AcEP and oPyAcEP were even more toxic in J774 cells. However, the latter fact does not completely exclude these compounds as potential antileishmanial drugs as long as they have sufficient activity against *Leishmania*. A good example in this respect is amphotericin B, which is highly toxic against mammalian cells. Nevertheless, its liposomal formulation is effectively used to treat leishmaniasis in humans. However, the study these pharmacokinetic influencing factors goes far beyond the possibilities of our simple in vitro models and cannot be studied with our methods.

Another group of compound pairs is characterized by antileishmanial activities of both the EP and their non-peroxidic analogs (Table 4). This group includes pairs, such as mPyBuAc/mPyBuAcEP and pPyBuAc/pPyBuAcEP. For these compounds also the non-peroxidic structure shows significant antileishmanial activity and exhibits a high activity against *Leishmania* and reduced toxicity in J774 cells resulting in a remarkable selectivity. These results indicate that in those molecules not only the peroxide group, but also other pharmacophores are probably involved in the antileishmanial action, which provide more selectivity.

To get more insights about the mechanism of action of these compounds in *Leishmania*, we studied their influence on the mitochondrial superoxide radical formation in *Leishmania* using the cyclic hydroxyl amine CMH and EPR spectroscopy for detection. The results demonstrate that antimycin A, an inhibitor of mitochondrial complex III, reliably triggers superoxide formation in *Leishmania*. Among the AcEPs and non-peroxidic analogs no clear indication that the endoperoxide group leads to superoxide formation in all AcEPs was observed (Figure 16).

To explore the chemical background of this biological activity, some AcEPs and their analogs were studied for their reactivity with low molecular iron (II) and their ability to undergo

cycloreversion by release of singlet oxygen. The reactivity with iron (II) was studied by formation of iron (III) and its complex formation with xylenol orange (Figure 17). This reagent forms a colored complex that can be detected at 560 nm in the visible spectrum. From the time course of this complex formation the reaction rates were calculated and displayed in the logarithmic scale in Figure 19. In most cases it became visible that the EPs reacted faster with iron (II) than the corresponding non-peroxidic analogs. This clearly indicates that EPs in *Leishmania* will interact with low molecular iron and result in radical formation and antileishmanial activity. An exception to this general behaviour was pPyBuAcEP and pPyBuAc for so far unknown reasons.

The ability of EPs to undergo cycloreversion (Figure 20) was studied at 70°C in ethanol as solvent. The results indicate that some of AcEPs are converted back to their corresponding Ac (Figures 24-25, Table 5). According to the literature this is accompanied by the release of singlet oxygen (Fudickar and Linker 2018). This group included the compounds, such as DPAcEP, mPyAcEP and pPyBuAcEP.

However, another group of AcEPs obviously did not convert back to their parent compound during thermal decomposition. This suggests that their thermal decomposition is based on more complex reaction mechanisms. This group included compounds, such as Ac1130EP and oPyAcEP (Table 5).

So far, the limited number of compound pairs studied in this work does not allow solid conclusions how these different reaction mechanisms are related to different biological activities.

In summary, this thesis established essential new methods to screen antileishmanial compounds more efficiently and to provide approaches to study possible synergies of antileishmanial compounds. Furthermore, the mechanistic experiments demonstrate that even among AcEPs the reaction mechanisms and possibly their biological activities can be achieved by very different pathways resulting in considerable different efficiency and selectivity in the system *Leishmania*/macrophages. Future studies will continue to explore these interesting initial findings.

5. Summary

Leishmaniasis is a vector-borne disease of tropical and subtropical countries. It is caused by protozoal parasites, which upon infection of mammals hide in host macrophages. Depending on the *Leishmania* species this infection can lead to skin and mucocutaneous lesions and even to death. Pharmacological therapy is difficult due to the location of the parasites inside the macrophage phagolysosome. Therefore, the exploration of new anti-leishmanial compounds and possible drug combinations are of general interest. In the current bachelor thesis, the influence of newly synthesized anthracene endoperoxides (AcEP) and the non-endoperoxide analogs (Ac) on non-pathogenic *Leishmania tarentolae* promastigotes (LtP) and J774 cells as model for host macrophages was studied. The work consisted of a methodical part, in which new testing methods were established, and an explorative part, in which antileishmanial properties and mechanism of AcEP were studied.

Major parts were (I) to establish refined methods for viability testing as well as methods to test the synergy of potential antileishmanial compounds, (II) to measure the effects of the AcEP/Ac compound set on the viability of LtP and J774 cells as well as their potential to trigger superoxide radical formation in LtP and (III) to characterize the compound set for its reactivity with low-molecular weight iron and their potential to undergo cycloreversion.

As results of this work a new viability plate layout giving up to 12 instead of 6 concentration points for concentration-viability curves and a plate layout for synergy testing of two compounds was established. Among the tested compounds certain AcEPs showed antileishmanial activity with IC_{50} values in the low micromolar range and selectivity for LtP versus J774 cells. By using cyclic hydroxyl amines in combination with EPR spectroscopy it was shown that some of these AcEP but also non-peroxidic analogs (Ac) triggered superoxide formation in LtP. In the chemical part of the study, it was shown that most of the AcEP reacted faster with low-molecular weight iron (II) than their non-peroxidic analogs (Ac). During the study of thermal degradation of the AcEP compounds at 70°C in ethanol it was shown that especially complex structured AcEP underwent cycloreversion (release of O₂) while simpler AcEPs also decomposed under these conditions, however, not under re-formation of their parent compound (no cycloreversion). In conclusion this work shows that antileishmanial activity of AcEP strongly depends on the structure beyond the endoperoxide group, which results in partially different biological effects in LtP. Furthermore, the decomposition of the endoperoxide group by iron or cycloreversion is often a prerequisite for their activity but is not strictly correlated with their effects on LtP viability. This work improved our understanding of the relation between endoperoxide structure and their antileishmanial activity.

6. Zusammenfassung

Leishmaniose ist eine wichtige Krankheit in tropischen und subtropischen Ländern. Sie wird durch Protozoen Parasiten verursacht, die sich bei Infektion von Säugetieren in Wirtsmakrophagen verstecken. Abhängig von der *Leishmania*-Spezies kann diese Infektion zu Haut- und Schleimhautläsionen und sogar zum Tod führen. Die pharmakologische Therapie ist aufgrund der Lage der Parasiten im Phagolysosom von Makrophagen limitiert. Deswegen ist die Erforschung neuer antileishmanialer Medikamente und möglicher Arzneimittelkombinationen von allgemeinem Interesse. In der aktuellen Bachelorarbeit wurde der Einfluss neu synthetisierter Anthracen-Endoperoxide (AcEP) und der Nicht-Endoperoxid-Analoga (Ac) auf *Leishmania tarentolae* Promastigoten (LtP) und J774-Zellen als Modell für Wirtsmakrophagen untersucht. Die Arbeit bestand aus einem methodischen Teil, in dem neue Testmethoden etabliert wurden, und einem explorativen Teil, in dem die antileishmanialen Eigenschaften und der Mechanismus der AcEPs untersucht wurden. Hauptbestandteile waren (I) die Festlegung neuer Methoden für Zellviabilität sowie Methoden zum Testen der Synergie potenzieller antileishmanialer Arzneimittel, (II) die Messung der Auswirkungen der AcEP / Ac-Verbindung auf die Zellviabilität von LtP- und J774-Zellen sowie ihr Potenzial, die Bildung von Superoxidradikalen in LtP auszulösen, ihre Reaktivität mit niedermolekularem Eisen zu reagieren und ihr Potenzial zur Cycloreversion zu charakterisieren. Als Ergebnis dieser Arbeit wurde ein neues Layout der Zellviabilität-Tests mit 12 statt 6 Konzentrationspunkten für Dosis-Wirkungs-Kurven und ein Plattenlayout für Synergie Zellviabilität-Tests von zwei Verbindungen erstellt. Unter den getesteten Verbindungen zeigten bestimmte AcEPs eine antileishmaniale Aktivität mit IC_{50} -Werten im niedrigen mikromolaren Bereich und Selektivität für LtP gegenüber J774-Zellen. Durch die Verwendung von cyclischen Hydroxylaminen in Kombination mit EPR konnte gezeigt werden, dass einige dieser AcEP-, aber auch der Nicht-Endoperoxid- Analoga, die Bildung von Superoxid Radikalen in LtP auslösten. Im chemischen Teil der Studie wurde gezeigt, dass der größte Teil des AcEP schneller mit Eisen (II) reagierte als ihre Ac. Während der Untersuchung des thermischen Abbaus der AcEP-Verbindungen bei 70 ° C in Ethanol wurde festgestellt, dass besonders komplexes AcEPs eine Cycloreversion (Freisetzung von O_2) durchliefen, während sich unter diesen Bedingungen auch einfachere AcEPs zersetzten, jedoch nicht unter Rückbildung ihrer Vorläufer-Verbindung (keine Cycloreversion). Zusammenfassend zeigt diese Arbeit, dass die antileishmaniale Aktivität von AcEPs stark von der Struktur jenseits der Endoperoxidgruppe abhängt, was zu unterschiedlichen biologischen Wirkungen bei LtP führt. Darüber hinaus ist die Zersetzung der Endoperoxidgruppe durch Eisen oder Cycloreversion häufig eine Voraussetzung für ihre Aktivität, korreliert jedoch nicht streng mit ihren Auswirkungen auf die Zellviabilität von LtP.

Diese Arbeit verbesserte unser Verständnis über der Beziehung zwischen der Struktur von EPs und ihrer antileishmanialen Aktivität.

7. Abbreviations

AA	...	Antimycin A
Ac	...	Anthracene
AcEP	...	Anthracene endoperoxide
ACN	...	Acetonitril
AmB	...	Amphotericin B
Asc	...	Ascaridole
BHI	...	Brain heart infusion medium
CDC	...	Centers for Disease Control and Prevention
CIA	...	Cell image analysis
CMH	...	Hydroxyl-3-methoxycarbonyl-2,2,5,5-tetramethylpyrrolidine hydrochloride
COX	...	Cyclooxygenase
DFO	...	Deferoxamine
DMEM	...	Dulbecco's modified eagle's medium
DMPO	...	5,5-dimethyl-1-pyrroline N-oxide
DMSO	...	Dimethyl sulfoxide
DTPA	...	Diethylenetriaminepentaacetic acid
EDTA	...	Ethylenediaminetetraacetic acid
EP	...	Endoperoxides
EPR	...	Electron paramagnetic resonance
FCS	...	Fetal calf serum
FIC	...	Fractional inhibitory concentration
GP63	...	Zinc-dependent metalloprotease
GPI	...	Glycosylphosphatidylinositol
HASP	...	Acylated surface proteins
IC ₅₀	...	Half maximal inhibitory concentrations
IL	...	Intralymphatic
IM	...	Intramuscular
Ipp	...	peak-to-peak Intensity
ISP	...	Inhibitors of serine peptidase
IV	...	Intravenous
LACK	...	Leishmania activated C kinase
LB	...	Lipid body
LIP	...	Labile iron pool
LPG	...	Lipophosphoglycan
LtP	...	Leishmania tarentolae promastigotes

MIL	...	Miltefosine
OD	...	Optical density
PBS	...	Phosphate buffered saline
Pen	...	Pentamidine
PMA	...	Phorbol-12myristate-13-acetate
PV	...	Parasitophorus vacuole
ROS	...	Reactive oxygen species
SD	...	Standard deviation
WHO	...	World Health Organization
XO	...	Xylenol orange
YE	...	Yeast extract

8. References

- Bates PA. 2018. Revising Leishmania's life cycle. *Nature Microbiology*, 3(5):529–530.
- Bell CA, Hall JE, Kyle DE, Grogl M, Ohemeng KA, Allen MA, Tidwell RR. 1990. Structure-activity relationships of analogs of pentamidine against *Plasmodium falciparum* and *Leishmania mexicana amazonensis*. *Antimicrobial Agents and Chemotherapy*, 34(7):1381–1386.
- Cao L, Jiang W, Cao S, Zhao P, Liu J, Dong H, Guo Y, Liu Q, Gong P. 2019. In vitro leishmanicidal activity of antimicrobial peptide KDEL against *Leishmania tarentolae*. *Acta Biochimica et Biophysica Sinica*, 51(12):1286–1292.
- Centers for Disease Control and Prevention. 2021. Leishmaniasis - Diagnosis. <https://www.cdc.gov/parasites/leishmaniasis/diagnosis.html> (accessed May 16, 2021).
- Clark DE. 2000. Peroxides and peroxide forming compounds (pdf), <https://www.bnl.gov/esh/cms/PDF/peroxides.pdf> (accessed May 14, 2021).
- Cokol-Cakmak M, Bakan F, Cetiner S, Cokol M. 2018. Diagonal method to measure synergy among any number of drugs. *Journal of Visualized Experiments*, (136):e57713.
- Fritsche CLE. 2008. Untersuchungen zur optimalen Kultivierung von *Leishmania tarentolae* [Dissertation]. Halle (Saale): Martin-Luther-Universität Halle-Wittenberg.
- Fudickar W, Linker T. 2018. Release of singlet oxygen from aromatic endoperoxides by chemical triggers. *Angewandte Chemie International Edition*, 57(39):12971–12975.
- Geroldinger G, Tonner M, Fudickar W, De Sarkar S, Dighal A, Monzote L, Staniek K, Linker T, Chatterjee M, Gille L. 2018. Activation of anthracene endoperoxides in *Leishmania* and impairment of mitochondrial functions. *Molecules*, 23 (7):1680.
- Geroldinger G, Tonner M, Hettegger H, Bacher M, Monzote L, Walter M, Staniek K, Rosenau T, Gille L. 2017. Mechanism of ascaridole activation in *Leishmania*. *Biochemical Pharmacology*, 132:48–62.
- Gupta S, Nishi S. 2011. Visceral leishmaniasis: experimental models for drug discovery. *The Indian Journal of Medical Research*, 133(1):27–39.
- Hossein R, Mohammad M. 2015. An overview on *Leishmania* vaccines: A narrative review article. *Veterinary Research Forum*, 6(1):1-7.
- Jefford CW. 1996. Six-membered rings with 1,2,4-oxygen or sulfur atoms. In: Katritzky AR, Rees CW, Scriven EFV (Eds.), *Comprehensive Heterocyclic Chemistry II. A review of the*

- literature 1982-1995: the structure, reactions, synthesis, and uses of heterocyclic compounds. Vol. 6. 1st edition. Oxford, New York: Pergamon, 861–899.
- Klatt S, Simpson L, Maslov DA, Konthur Z. 2019. *Leishmania tarentolae*: taxonomic classification and its application as a promising biotechnological expression host. *PLoS Neglected Tropical Diseases*, 13 (7):7424.
- Kobets T, Grekov I, Lipoldova M. 2012. Leishmaniasis: complexity at the host-pathogen interface. *Current medicinal chemistry*, 19(10):1443–1474.
- Loría-Cervera EN, Andrade-Narváez FJ. 2014. Animal models for the study of leishmaniasis immunology. *Revista do Instituto de Medicina Tropical de Sao Paulo*, 56(1):1–11.
- Madhvi A, Mishra H, Leisching GR, Mahlobo PZ, Baker B. 2019. Comparison of human monocyte derived macrophages and THP1-like macrophages as in vitro models for *M. tuberculosis* infection. *Comparative Immunology, Microbiology and Infectious Diseases*, 67:101355.
- Menezes JPB, Guedes CES, Petersen ALOA, Fraga DBM, Veras PST. 2015. Advances in development of new treatment for leishmaniasis. *BioMed Research International*, 2015:815023.
- Monzote L, García M, Pastor J, Gil L, Scull R, Maes L, Cos P, Gille L. 2014. Essential oil from *Chenopodium ambrosioides* and main components: activity against *Leishmania*, their mitochondria and other microorganisms. *Experimental Parasitology*, 136:20–26.
- Müllebnner A, Patel A, Stamberg W, Staniek K, Rosenau T, Netscher T, Gille L. 2010. Modulation of the mitochondrial cytochrome bc1 complex activity by chromanols and related compounds. *Chemical Research in Toxicology*, 23(1):193–202.
- Ortega V, Giorgio S, Paula E. 2017. Liposomal formulations in the pharmacological treatment of leishmaniasis: a review. *Journal of Liposome Research*, 27(3):234–248.
- Palma E, Pasqua A, Gagliardi A, Britti, D, Fresta M, Cosco D. 2018. Antileishmanial activity of amphotericin B-loaded-PLGA nanoparticles: An Overview. *Materials*, 11(7):1167
- Petitdidier E, Pagniez J, Pissarra J, Holzmüller P, Papierok G, Vincendeau P, Lemesre J, Bras-Gonçalves R. 2019. Peptide-based vaccine successfully induces protective immunity against canine visceral leishmaniasis. *NPJ Vaccines*, 4:49.
- Podinovskaia M, Descoteaux, A. 2015. *Leishmania* and the macrophage: a multifaceted interaction. *Future Microbiology*, 10(1):111–129.

- Ricciotti E, FitzGerald GA. 2011. Prostaglandins and inflammation. *Arteriosclerosis, Thrombosis, and Vascular Biology*, 31(5):986–1000.
- Santarém N, Tavares J, Cordeiro-da-Silva A. 2019. In vitro infections of macrophage-like cell lines with *Leishmania infantum* for drug screening. *Methods in Molecular Biology*, 1971:265–277.
- Scariot DB, Britta EA, Moreira AL, Falzirolli H, Silva CC, Ueda-Nakamura T, Dias-Filho BP, Nakamura CV. 2017. Induction of early autophagic process on *Leishmania amazonensis* by synergistic effect of miltefosine and innovative semi-synthetic thiosemicarbazone. *Frontiers in Microbiology*, 8:255.
- Sebaugh JL. 2011. Guidelines for accurate EC50/IC50 estimation. *Pharmaceutical Statistics*, 10(2):128–134.
- Singh N, Kumar M, Singh RK. 2012. Leishmaniasis: current status of available drugs and new potential drug targets. *Asian Pacific Journal of Tropical Medicine*, 5(6):485–497.
- Sunter J, Gull K. 2017. Shape, form, function and *Leishmania* pathogenicity: from textbook descriptions to biological understanding. *Open Biology*, 7(9):170165.
- Torres-Guerrero E, Quintanilla-Cedillo MR, Ruiz-Esmenjaud J, Arenas R. 2017. Leishmaniasis: a review. *F1000Research*, 6:750.
- Tran T, Qiao Y, You H, Cheong DHJ. 2018. Chronic inflammation in asthma: antimalarial drug artesunate as a therapeutic agent. In: Chatterjee S, Jungraithmayr W, Bagchi D (Eds.): *Immunity and Inflammation in Health and Disease*. 1st edition. London, New York, Cambridge, Oxford: Academic Press, 309–318.
- World Health Organization. 2021. Leishmaniasis. <https://www.who.int/news-room/fact-sheets/detail/leishmaniasis> (accessed May 14, 2021)
- World Health Organization. 2019. Status of endemicity of visceral leishmaniasis worldwide, 2019. https://cdn.who.int/media/docs/default-source/ntds/leishmaniasis/leishmaniasis-vl-2019.pdf?sfvrsn=a9c1920e_9 (accessed May 16, 2021).
- World Health Organization. 2019. Status of endemicity of cutaneous leishmaniasis worldwide, 2019. https://cdn.who.int/media/docs/default-source/ntds/leishmaniasis/leishmaniasis-cl-2019.pdf?sfvrsn=7b1eedab_7 (accessed May 16, 2021).
- Zahid MSH, Johnson MM, Tokarski RJ, Satoskar AR, Fuchs JR, Bachelder EM, Ainslie KM. 2019. Evaluation of synergy between host and pathogen-directed therapies against

intracellular *Leishmania donovani*. *International journal for parasitology. Drugs and drug resistance*, 10:125–132.

Zurier RB. 2017. Prostaglandins, leukotrienes, and related compounds. In: Firestein GS, Budd RC, Gabriel SE, McInnes IB, O'Dell JR (Eds.), *Kelley and Firestein's Textbook of Rheumatology*. Tenth edition. Philadelphia, PA: Elsevier, 366-383.e3.

9. List of figures

Figure 1. Status of endemicity of visceral leishmaniasis worldwide.....	2
Figure 2. Status of endemicity of visceral leishmaniasis worldwide.....	3
Figure 3. Morphological structures of a promastigote and an amastigote (Sunter and Gull 2017)	4
Figure 4. The life cycle of Leishmania.(Sunter and Gull 2017)	5
Figure 5. (A) AmB and miltefosine show mild synergetics effects, while (B) paromomycin with AmB showed additive interaction in low doses and antagonism in higher doses. (Zahid et al. 2019)	14
Figure 6. Structures and abbreviations of AcEPs, their corresponding Ac, Pen (control substance) and AA	16
Figure 7. Vertical serial dilution viability assay	19
Figure 8. Horizontal serial dilution viability assay	20
Figure 9. Combination viability assay	21
Figure 10. Concentration-viability curve of combination viability of as a function of different concentrations of Mil (left) (15 μ M - 0.029 μ M) and mPyBuAcEP (right) (100 μ M - 0.195 μ M)	25
Figure 11. Concentration-viability curve of Mil in combination and mPyBuAcEP in combination represent the effect on IC ₅₀ values of each compound in combination.....	25
Figure 12. Concentration-viability curve of the horizontal viability assay of LtP as a function of different concentrations of Ac1130 (left) (from 200 μ M to 0.098 μ M) and its EP (right) (from 20 μ M to 0.01 μ M)	26
Figure 13. Concentration-viability curve of the horizontal viability assay of J774 macrophages as a function of different concentrations of Ac1130EP (left) (0.06 μ M, 0.32 μ M, 1.60 μ M, 8.00 μ M, 40 μ M, 200 μ M) and its corresponding non-EP (right), (Ac1130EP 0.06 μ M, 0.32 μ M, 1.60 μ M, 8.00 μ M, 40 μ M, 200 μ M)	26
Figure 14. Reaction of CMH with superoxide radicals O ₂ [•] forming the stable radical CM [•] , detected by EPR spectroscopy	28
Figure 15. EPR spectrum of CM [•] obtained from CMH oxidation. The peak-to-peak intensity (I _{pp}) which was used for quantification is indicated	28
Figure 16. CMH oxidation (% of LtP) in the presence of AA or Ac (A: Ac1130 B: Ac1118; C: pPyBuAc; D: oPyAc; E: DPAC; F: AcEP; G: mPyBuAcEP) or AcEP (A: Ac1130EP; B: Ac1118EP; C: pPyBuAcEP; D: oPyAcEP; E: DPACEP; F: oPy2C8AcEP; G : mPyBuAcEP) (each 100 μ M). PBS/Glucose represents a control experiment without LtP	30
Figure 17. The reaction of AcEP decomposition by Fe ²⁺ . Fe ²⁺ triggers AcEP cleavage into radical products and Fe ³⁺	31

Figure 18. The spectra of the XO/ Fe ³⁺ complex formation in the presence of 100 μM oPyAcEP	31
Figure 19. Formation rate of the xylenol/Fe ³⁺ complex by EPs (final concentration 100 μM) Data represent mean ± SD of three experiments.....	32
Figure 20. The concept of AcEP undergoing cycloreversion and releasing singlet oxygen by heating	32
Figure 21. UV spectra of DPAC (top) (8 μM) and DPACEP (bottom) (40 μM) after heating for 0, 6, 12, 18 and 22 h	33
Figure 22. UV spectra of Ac1130 (top) (8 μM) and Ac1130EP (bottom) (40 μM) after heating for 0, 6, 12, 18 and 21 h	34
Figure 23. UV spectra of mPyBuAc (top) (2 μM) and mPyBuAcEP (bottom) (40 μM) after heating for 0, 6, 12, 18 and 23 h	35
Figure 24. UV spectra of oPyAc (top) (8 μM) and oPyAcEP (bottom) (40 μM) after heating for 0, 6, 12, 18 and 23 h	36
Figure 25. UV spectra of pPyBuAc (top) (8 μM) and pPyBuAcEP (bottom) (40 μM) after heating for 0, 6, 12, 18 and 23 h	37

10. List of tables

Table 1. The vector, disease and origin of different Leishmania species.	2
Table 2. List of chemicals used for sample preparation and maintenance work.	15
Table 3. IUPAC names of AcEPs and their corresponding non-endoperoxides used in this work.	17
Table 4. IC ₅₀ values and selectivity of EPs and their corresponding non-EPs in LtP and J774 cells. The IC ₅₀ values were determined by using resazurin viability assay in 96 well plates. Data represent mean ± SD of 3-9 individual experiments.	27
Table 5. EPs studied and their ability to undergo cycloreversion based on the UV Spectra of the EPs and their corresponding non-EPs.	38